Individuals born with congenital cataracts exhibit both persisting impairment and considerable recovery of white matter microstructure after sight restoration

Jordan D. Hassett[1,2], Cordula Hölig[1], Sunitha Lingareddy[3], Ramesh Kekunnaya[4] & Brigitte Röder[1,4]

[1] *Biological Psychology und Neuropsychology, University of Hamburg, Hamburg, Germany*
[2] *Max Planck School of Cognition, Leipzig, Germany*
[3] *Lucid Medical Diagnostics, Hyderabad, India*
[4] *Jasti V Ramanamma Children's Eye Care Center, Child Sight Institute, LV Prasad Eye Institute, Hyderabad, India*

Corresponding author:
Jordan Hassett
Biological Psychology and Neuropsychology
University of Hamburg
Von Melle Park 11
20146 Hamburg
Germany
Email: jordan.hassett@maxplanckschools.de

Abstract

Introduction

Individuals born with dense bilateral cataracts, for whom sight was restored later in life (congenital cataract reversal individuals), provide a unique opportunity to explore the impact of early (visual) experience on the development of the human brain.

Methods

Using diffusion MRI we assessed white matter microstructure in a sample of 20 congenital cataract reversal individuals using along-the-tract analysis of major visual white matter tracts and non-visual control tracts. We additionally recruited three control groups: 8 permanently congenitally blind individuals, 11 individuals with reversed later-onset cataracts (developmental cataract reversal individuals), and 24 age- and sex-matched typically sighted controls.

Results

Diffusion tensor metrics exhibited significant group differences which were specific to visual tracts. Compared to normally sighted controls, congenitally blind and congenital cataract reversal individuals both showed impaired white matter integrity. However, differences were much more spatially extensive for permanently congenitally blind individuals, and a direct comparison revealed relatively higher tract integrity for congenital cataract reversal individuals, suggesting a high degree of recovery following sight restoration.

Discussion

The present pattern of results is compatible with the idea of both a sensitive period for white matter development and significant white matter plasticity later in life. We propose that group differences are largely driven by differences in myelination. Thus, the considerable recovery in

congenital cataract reversal individuals would suggest that life-long myelin plasticity may remain higher than neuronal structural plasticity.

Keywords: Tractography, diffusion-weighted imaging, sensitive period, congenital cataract, sight recovery, visual system, brain development, myelin plasticity

Introduction

While brain development is a lengthy process that continues into young adulthood, the first years of life seem to be particularly important, highlighted by remarkable neural changes that are especially relevant to function. In addition to the guiding role of genes, postnatal brain development is heavily dependent on experience [1,2]. The term 'sensitive periods' refers to epochs in life where brain development is especially susceptible to experience; a lack of, or aberrant experience during this phase cannot be fully reversed later in life [3]. This is distinctly evident for neural circuits in the visual system. The pioneering work of Hubel and Wiesel [4] established in non-human animal models that a sensitive period exists for visual development. More recent studies have taken this a step further, defining multiple sensitive periods for different visual functions in non-human animals [5,6] and humans [7–9]. The existence of such sensitive periods would suggest that early visual deprivation can considerably and permanently alter neural developmental trajectories in the visual system.

In humans, natural models for investigating the role of early visual experience on brain development are scarce. Traditionally, the impact of congenital vs. late visual deprivation on functional and structural brain organisation has been investigated in permanently blind humans [10–13]. While this research allows conclusions about sensitive periods for atypical brain development, that is, the capacity of the brain to adapt to an unexpected environment, conclusions about sensitive periods for typical brain development are not possible [13]. Thus, individuals who were born blind but recovered sight later in life must be investigated to explore whether the neural circuits can make up for the lack of early experience later in life. After undergoing cataract removal surgery, people born with dense bilateral cataracts (opaque lenses) provide such an opportunity. Clinical research in this group has consistently reported visual

acuity deficits [14,15]. Cognitive neuroscience work has extended these clinical observations to higher visual functions such as coherent motion [16] and face processing [17–19]. Despite permanent visual deficits, considerable recovery of other functions, such as biological motion and color processing, has been demonstrated as well [16,20–24]. Though limited, recent neuroimaging efforts have begun to explore the neural correlates of sight restoration after congenital visual deprivation . For instance, visual cortical morphometry (e.g. gray matter thickness and cortical surface area) was found to not recover following sight restoration [25–27]. Other studies have reported altered retinotopic organization [28] and excitation/inhibition profiles in the visual cortex [29,30] in individuals with reversed congenital cataracts.

Diffusion magnetic resonance imaging (MRI) can be used to compute metrics that approximate white matter microstructure: Fractional anisotropy (FA) measures the fraction of diffusion that is directional, while mean diffusivity (MD), radial diffusivity (RD) and axial diffusivity (AD), quantify the magnitude of diffusion directionally averaged, perpendicular, and parallel to fiber tracts, respectively. Despite widespread application, the neurobiological underpinnings of these diffusion metrics remain somewhat ambiguous [31]. Generally speaking, impaired white matter integrity has been associated with increased MD and RD, and decreased FA and AD. More specifically, while FA is highly sensitive to microstructural changes, it is neurobiologically nonspecific (e.g., has been related to myelin and axonal density, or in clinical cases to inflammation and edema) [31,32]. MD reflects the overall magnitude of diffusion and is nonspecific as well (e.g. changes can reflect differences in cell density or be linked to inflammation, edema or necrosis in clinical cases) [32]. In contrast, RD and AD feature much more specificity; RD is

thought to be inversely linked to myelination [32,33], while lower AD seems to reflect reduced axonal integrity [33,34].

There is no shortage of literature surrounding DTI in permanent blindness [11]. Most studies agree that there is decreased white matter integrity in the optic radiation as a result of blindness [10,35–44]. However, the secondary findings of these studies demonstrate considerable variation. For instance, the time of onset may indeed be important for white matter microstructure, but there is some disagreement as to the exact effect. Some studies found that the optic radiation remains relatively intact for late-blind compared to early-blind individuals [35,41], while another study instead suggested that the optic radiation may actually be more degraded in late-blind than early-blind individuals [36]. Looking at other regions, disparity also exists; where a reduction in FA in the splenium has been reported [38,40,44], other research has found this not to be the case [42,45]. Studies have additionally found decreased white matter integrity in late visual tracts of the ventral stream like the inferior longitudinal fasciculus and inferior frontal-occipital fasciculus [10,38,42,46], with less support for similar differences in the dorsal stream via the superior longitudinal fasciculus [10]. In summary, white matter imaging studies in permanently congenitally blind humans have consistently observed changes, including decreased FA and increased MD, in early visual tracts. Additionally, some studies have reported similar changes in higher order visual areas, including tracts of the ventral and dorsal stream (for a recent summary see Paré et al. 2023 [11]).

In the only study investigating white matter integrity in congenital cataract reversal individuals [47], the authors employed a longitudinal approach to quantify the effect of sight restoring surgery

on mean FA and MD in ten early-visual, late-visual and non-visual tracts. These authors found significant surgery-related recovery in late-visual tracts, but surprisingly, they did not observe significant changes from pre- to post-surgery assessments in either the optic tract or optic radiation. In a cross-sectional analysis however, Pedersini et al. (2023) [47] additionally found group differences between post-surgery MD values relative to a dataset retrieved from the Human Connectome Project, as the authors themselves had not scanned normally sighted control subjects.

In the present study, we used diffusion tractography to assess white matter integrity in major visual tracts for a large sample of congenital cataract reversal individuals. We opted for a more granular 'along-the-tract' analysis, considering that metric values are known to naturally vary along the length of a tract [31,48]. Furthermore, we additionally assessed RD and AD metrics to better unravel possible mechanisms of white matter impairments in this group. We took a cross-sectional approach involving an age- and sex-matched normally sighted control group, as well as permanently congenitally blind individuals and individuals with reversed developmental (later-onset) cataracts all recruited from the same community and scanned in the same facility. Using this approach, we hoped to isolate the effects of sight restoration after congenital visual deprivation (as opposed to permanent congenital blindness). We expected that visual tract profiles would be significantly altered in congenital cataract reversal individuals relative to normally sighted and permanently congenitally blind individuals. Specifically, we hypothesized that diffusion tensor metrics would indicate reduced white matter integrity in visual tracts for congenital cataract reversal individuals compared with normally sighted controls. However, considering the observed partial functional recovery in congenital cataract reversal individuals

[21,24,49,50], we predicted that sight restoration had induced white matter plasticity, resulting in increased integrity in congenital cataract reversal individuals compared to permanently congenitally blind individuals. Similarly, although Pedersini et al. (2023) [47] were unable to find longitudinal changes in early-visual tracts, considering the extensive literature supporting the optic radiation as a primary tract affected by blindness [10,35–44], we anticipated that differences between congenital cataract reversal individuals and permanently congenitally blind individuals would reflect white matter plasticity in early-visual tracts related to sight restoration.

Methods

Participants

Using the same original dataset as Hölig et al. (2023) [25], additional participants were excluded (n=6) due to incomplete datasets (n=4, one congenital cataract reversal individual, three sighted controls) and issues in preprocessing (n=2, both congenitally blind individuals), leaving a final sample of 63 participants. The primary study group consisted of 20 individuals (mean age (SD) [range] = 19 (10) [6-36] years, 50% female) born with dense bilateral cataracts, surgically removed later in life (mean age at surgery (SD) [range] = 8 (9) [3 months – 31] years), henceforth referred to as congenital cataract reversal individuals (CC). The existence of congenital dense, total bilateral cataract was affirmed by a team of ophthalmologists and optometrists based on medical history, the presence of sensory nystagmus and strabismus, absence of fundus view prior to surgery and a positive family history. Full participant details are reported in supplementary table 1.

Secondary groups included eight permanently congenitally blind individuals (CB) (mean age (SD) [range] = 21 (7) [16-39] years, 37.5% female) who were totally blind (no more than

rudimentary light perception) due to peripheral reasons, and 11 developmental cataract reversal individuals (DC) (mean age (SD) [range] = 16 (10) [9-43] years, 27.3% female). DC participants had a history of late onset childhood (developmental) cataracts and cataract surgery (mean age at surgery (SD) [range] = 13 (10) [7-40] years). No other sensory impairments or neurological disorders were reported by any of the participants. Full details are reported in supplementary tables 2 and 3 respectively.

A total of 24 typically sighted controls (SC) were recruited from the local community (mean age (SD) [range] = 20 (10) [6-42] years, 33.3% female). They were age- and sex-matched to CC, CB and DC participants; specifically, 16 were matched to CC individuals, eight to CB individuals, and 11 to DC individuals. Note that some SC subjects served as controls for multiple groups.

All visually impaired participants were recruited at the LV Prasad Eye Institute in Hyderabad, India. Image acquisition took place at the Lucid Medical Diagnostics radiological center in Banjara Hills in Hyderabad. Participants were given a small monetary compensation or a small gift (under age participants), and all associated costs with participating (e.g., travel, accommodation, etc.) were reimbursed. Written informed consent (orally translated into language the participant or legal guardian was able to understand) was obtained from each participant or their legal guardian prior to scanning. This study was jointly approved by the institutional ethics review board of the LV Prasad Eye Institute in Hyderabad, India, as well as the ethics commission of the German Psychological Society.

Image Acquisition

All magnetic resonance imaging was performed using a 1.5T GE Signa HDxt scanner (GE Healthcare, Milwaukee, Wisconsin, USA) with an 8-channel head coil at the Lucid Medical Diagnostics radiological clinic in Banjara Hills, Hyderabad, India. Whole-brain diffusion weighted images were acquired with a 55-slice gradient-echo EPI2 sequence acquired in the sagittal plane, with 60 gradient directions (voxel size=0.9375mm x 0.9375mm x 2.5mm, interslice interval=2.5mm, TE=0.0936 s, TR=15.05 s, inversion time = 0, flip angle = 90 b-value = 1000 s/mm^2, FOV = 240 x 240 x 138 mm).

Image Processing

Initial diffusion image processing was performed using MRTrix3 (https://www.mrtrix.org/) [51]. Specifically, processing began with denoising, unringing to correct for Gibbs ringing artifacts, followed by motion and distortion correction. As reverse-phase encoded images were unavailable, synthetic ones were created using Synb0 (https://github.com/MASILab/Synb0-DISCO) [52,53]. A tensor was fitted to the preprocessed diffusion weighted image, and tensor metrics, FA, MD, RD, and AD, were then calculated for each voxel. Tensor images were registered to MNI-space, and 72 white matter tracts were segmented with TractSeg (https://github.com/MIC-DKFZ/TractSeg?tab=readme-ov-file) [54]. Of these 72 tracts, we selected a subset of 16, according to recent studies of individuals with visual impairments [10,38,46,47]. These included nine tracts related to vision; the optic radiation (OR; left and right), the splenium (corpus callosum), the inferior frontal occipital fasciculus (IFOF; left and right), the inferior longitudinal fasciculus (ILF; left and right), and the superior longitudinal fasciculus (specifically, the second division [55(p12)]; SLF; left and right). Seven additional tracts were chosen as negative controls; the genu (corpus callosum), the cerebrospinal tract (CST; left and right), the cingulum

(CG; left and right), and the uncinate fasciculus (UF; left and right). Tracking was performed on 10000 streamlines (a high number of streamlines reduces variability due to random seeding). We additionally used the built-in tractometry function of TractSeg [56,57], enabling what is commonly referred to as along-the-tract statistics. Each tract was resampled at 100 points along the length of the tract, and mean FA, MD, RD, and AD values were extracted at each of those points. While many studies, including the statistical analysis of Pedersini et al. (2023) [47], employed a 'tract average' approach, this might have obscured a wealth of important information; diffusion metrics vary considerably across tract profiles, as developmental or neuropathological changes will often occur in focal parts of a tract rather than uniformly across it and behavioural associations may show similar spatial specificity [48]. As such, an along-the-tract approach adds much-needed granularity and may improve sensitivity.

Statistics

Prior to group comparisons, a modified Z-score was used to probe each group for outliers (modified z-score ≥ 3) in any of the visual tracts and metrics. For all selected tracts, group means for diffusion metrics were calculated for each of 98 segments (100 – 2 end segments). Group means were compared using independent two-sample t-tests, creating four matrices (CC vs SC participants, CB vs SC participants, DC vs SC participants, CC vs CB participants) containing the T-statistics of 16 tracts x 98 segments. Multiple comparisons correction was performed by calculating a cluster size threshold. Specifically, a maximum-cluster-size null distribution was generated for each metric (FA, MD, AD, RD) and group comparison using 10,000 permutations to calculate the maximal number of consecutive segments within a tract that demonstrated significant ($p < 0.05$) group differences. The maximal cluster size at the 99.9th percentile of these

16 null distributions was taken as the cluster-size threshold. Observed clusters exceeding this threshold were considered significant, with a type 1 error rate of 0.001 or less.

Within each cluster, the sum of all T-statistics was taken as the cluster mass, in order to quantify the magnitude of the differences within each cluster. Additionally, in order to provide a metric of spatial specificity, the location of the cluster was recorded as the range of segments belonging to the cluster (numbered along the tract in an upstream manner (e.g. 1 is the most downstream segment)). Lastly, an average tract deviation metric was calculated for visual and non-visual tracts, by separately taking the sum of absolute values of all cluster masses for all visual tracts, and non-visual tracts respectively, then dividing by the number of tracts (nine and seven, respectively). This metric served two functions; first, summarize the total magnitude of differences between groups, and second, provide an indication of whether changes are global, or specific to visual tracts.

Artificial intelligence usage

No generative AI tools were used at any stage of the production of this manuscript.

Results

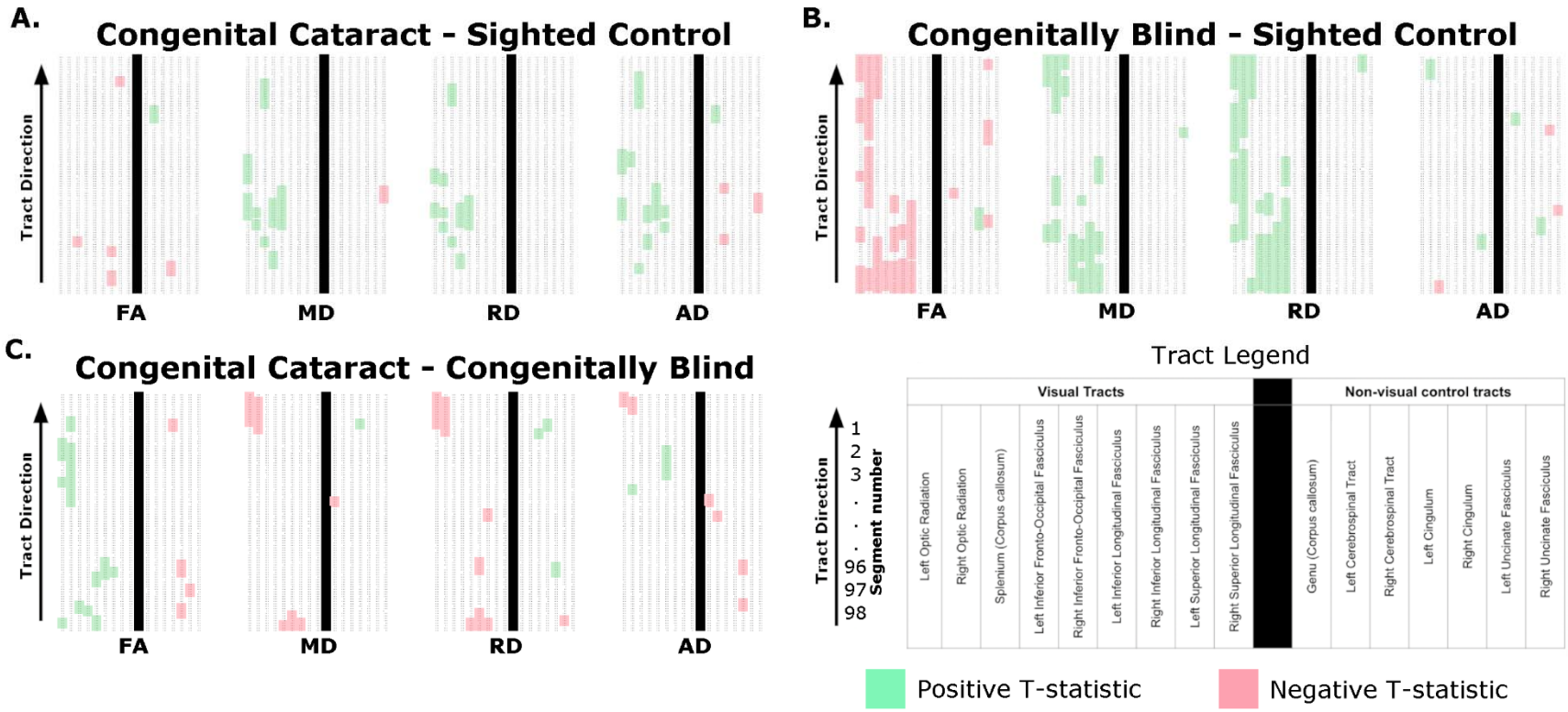

Figure 1: Overview of significant differences between groups. Each subplot shows significant differences in fractional anisotropy (FA), mean diffusivity (MD), radial diffusivity (RD) and axial diffusivity (AD) (labelled at the bottom). Each column represents a specific tract, for which 98 segments are displayed in rows, with downstream locations at the top. As indicated in the tract legend, tracts are organized from left to right as follows: Left Optic Radiation, Right Optic Radiation, Splenium, Left Inferior Fronto-Occipital Fasciculus, Right Inferior Fronto-Occipital Fasciculus, Left Inferior Longitudinal Fasciculus, Right Inferior Longitudinal Fasciculus, Left Superior Longitudinal Fasciculus, Right Superior Longitudinal Fasciculus, Genu, Left Corticospinal Tract, Right Corticospinal Tract, Left Cingulum, Right Cingulum, Left Uncinate Fasciculus, and Right Uncinate Fasciculus. The vertical black line indicates the separation of vision-related tracts (left) from non-visual control tracts (right). Clusters ($p < 0.001$) are coloured according to the direction of the difference. For example, in A, congenital cataract reversal individuals vs matched sighted controls, green clusters indicate that the respective tensor metric is significantly greater for the congenital cataract reversal group than for normally sighted controls, while red clusters indicate the opposite. This theme accordingly applies to B, permanently congenitally blind individuals vs matched sighted controls, and C, congenital cataract reversal individuals vs permanently congenitally blind individuals.

Group comparisons

Significant differences were found for all four group comparisons (CC vs SC, CB vs SC, DC vs SC, CC vs CB), primarily in visual tracts (Figure 1, Table 1). Below we report the results of comparisons between CC and matched SC participants, CB and matched SC participants, and CC and CB individuals for the left and right optic radiation, the splenium, the left and right IFOF, and the left and right ILF. We additionally provide a descriptive overview of cluster location, including spatial similarity across hemispheres and comparisons. Note that DC vs SC results and discussion can be found in the supplement (supplementary figure 1, supplementary table 4).

Table 1. Average tract deviations of visual and non-visual tracts for each comparison and metric.

	CC vs SC		CB vs SC		CC vs CB	
Metric	Visual	Non-visual	Visual	Non-visual	Visual	Non-visual
FA	4.44	4.31	95.72	11.68	24.21	8.59
MD	22.45	2.24	61.92	1.36	16.55	2.86
RD	17.88	0	109.05	2.80	19.83	7.08
AD	21.70	8.49	5.88	7.73	9.23	7.55

Table note: Average tract deviation is the mean sum of cluster masses, averaged separately across all visual, and all non-visual tracts. These scores are reported for each group comparison and tensor metric. Relatively larger values indicate that, on average, tracts showed a greater degree of differences between groups. CC – congenital cataract reversal individuals; CB – Permanently congenitally blind individuals; SC – Normally sighted control individuals; FA – Fractional anisotropy; MD – Mean diffusivity; RD – Radial diffusivity; AD – Axial diffusivity.

Optic Radiation

Compared to SC subjects, CB individuals exhibited significantly decreased FA and increased MD, RD and AD (figure 2B, table 2). Except for FA, similar patterns of differences were found

in CC compared to SC individuals (figure 2A, table 2). Comparing CC to CB participants directly revealed that FA was higher for CC individuals, while MD, RD and AD were lower (figure 2C, table 2). These differences mostly existed bilaterally, and many clusters appeared to show some degree of spatial overlap across hemispheres. Furthermore, some level of overlap was visible across comparisons, such that some significant CC vs SC and CC vs CB clusters were significant for CB vs SC too. However, there was very little apparent overlap between CC vs SC and CC vs CB comparisons.

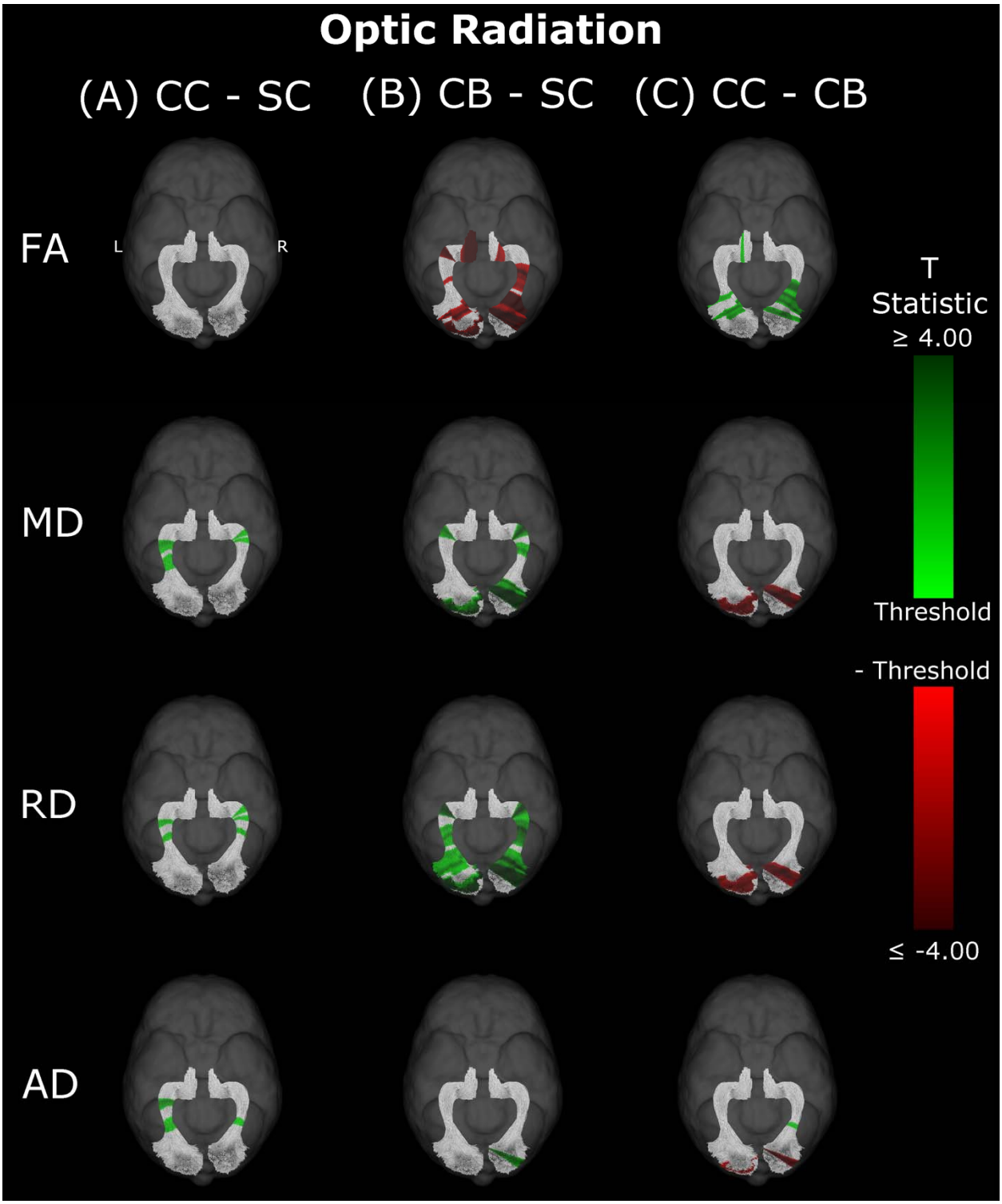

Figure 2: Group differences in FA, MD, RD and AD within the left and right optic radiations. The transposed segmentations of the left and right optic radiation are coloured according to the spatial location along the tract of clusters of significant differences between A) CC and SC individuals, B) CB and SC individuals, and C) CC and CB individuals. Segments coloured green indicate that the metric is higher in the first group than the second, while red segments specify the opposite. The shade of colour encodes the degree of difference, with light shades representing near-threshold T-statistics (2.032; 2.145; 2.056), and darker shades reflecting larger T-statistics. CC – congenital

cataract reversal individuals; CB – Permanently congenitally blind individuals; SC – Normally sighted control individuals; FA – Fractional anisotropy; MD – Mean diffusivity; RD – Radial diffusivity; AD – Axial diffusivity.

Table 2. Cluster masses and segment ranges for the left and right optic radiation, by group comparison, hemisphere, and metric.

Optic Radiation						
	CC vs SC		CB vs SC		CC vs CB	
Metric	Left	Right	Left	Right	Left	Right
FA			39.84 [1-11] 29.4 [19-28] 9.66 [49-52] 21.49 [72-77] 38.41 [88-98]	142.23 [1-35] 76.49 [39-63] 24.31 [89-97]	23.87 [20-28] 9.2 [36-39] 8.74 [94-97]	14.83 [11-16] 74.83 [22-47]
MD	26.11 [42-53] 25.68 [58-68]	8.37 [64-67] 8.77 [69-72]	43.37 [1-13] 20.62 [71-77]	87.02 [1-24] 30.15 [51-62] 28.93 [69-77]	42.36 [1-14]	47.15 [3-17]
RD	13.13 [48-53] 13.49 [62-67]	10.84 [50-54] 8.56 [64-67] 8.48 [70-73]	50.82 [1-14] 50.32 [21-40] 46.8 [44-61] 26.31 [71-77]	123.95 [1-34] 117.95 [40-76]	42.51 [1-15]	45.65 [3-18]
AD	22.11 [40-49] 23.9 [60-68]	12.62 [41-46]		22.8 [3-10]	15.59 [1-6]	21.71 [3-9] 8.78 [39-42]

Table note: Each entry refers to a cluster of significantly different segments found in the left or right optic radiation, organized by group comparison, hemisphere and tensor metric. Multiple entries refer to multiple clusters. Clusters are reported as 'cluster mass [segment range]'. CC – congenital cataract reversal individuals; CB – Permanently congenitally blind individuals; SC – Normally sighted control individuals; FA – Fractional anisotropy; MD – Mean diffusivity; RD – Radial diffusivity; AD – Axial diffusivity.

Splenium

In CB individuals, FA and AD were significantly decreased compared to SC participants, while MD and RD were significantly increased (figure 3B, table 3). Similarly, differences in all metrics were evidenced for CC compared to SC individuals, but with AD being increased rather than decreased (figure 3A, table 3). Direct CC to CB group comparisons revealed only one small cluster of higher FA for CC individuals in the right hemispheric portion of the tract (figure 3C,

table 3). Bilaterality can be partially observed, primarily in CC vs SC comparisons, with clusters in MD, RD and AD showing some degree of spatial similarity across hemispheres. Three significant clusters in CC vs SC comparisons for FA, MD and RD appeared to overlap with clusters in CB vs SC comparisons.

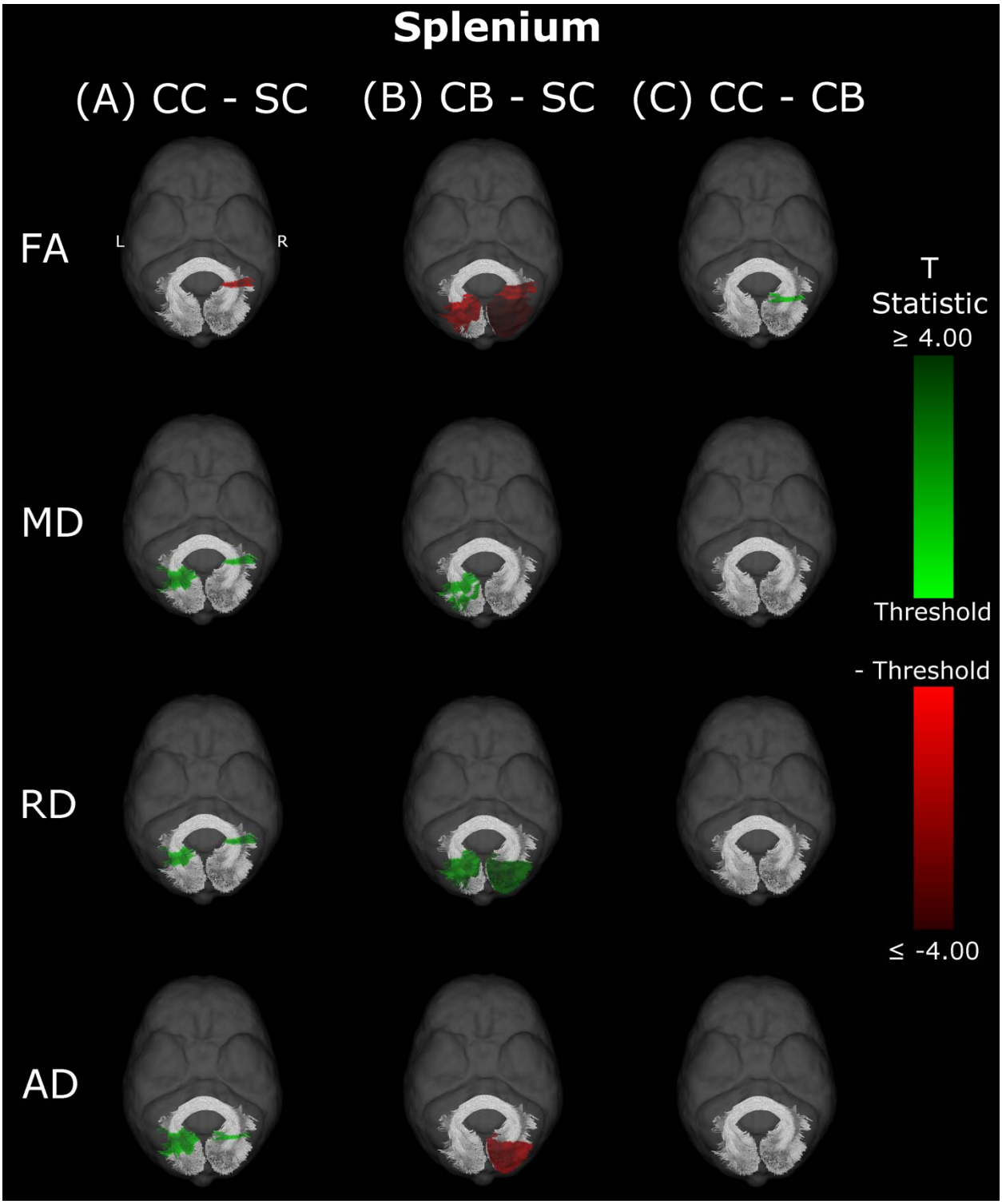

Figure 3: Group differences in FA, MD, RD and AD within the splenium. The transposed segmentation of the splenium is coloured according to the spatial location of clusters of significant differences between A) CC and SC individuals, B) CB and SC individuals, and C) CC and CB individuals. Segments coloured green indicate that the metric is higher in the first group than the second, while red segments specify the opposite. The shade of colour encodes the degree of difference, with light shades representing near-threshold T-statistics (2.032; 2.145; 2.056), and darker shades reflecting larger T-statistics. CC – congenital cataract reversal individuals; CB – Permanently

congenitally blind individuals; SC – Normally sighted control individuals; FA – Fractional anisotropy; MD – Mean diffusivity; RD – Radial diffusivity; AD – Axial diffusivity.

Table 3. Cluster masses and segment ranges for the splenium, by group comparison and metric.

Splenium			
Metric	CC vs SC	CB vs SC	CC vs CB
FA	9.58 [76-79]	50.36 [1-18] 95.47 [76-98]	10.58 [87-91]
MD	30.25 [11-22] 8.95 [76-79]	15.5 [1-6] 19.86 [10-17]	
RD	21.37 [13-21] 9.64 [76-79]	52.92 [1-18] 19.3 [93-98]	
AD	38.19 [8-22] 8.53 [87-90]	13.24 [94-98]	

Table note: Each entry refers to a cluster of significantly different segments found in the splenium, organized by group comparison and tensor metric. Multiple entries refer to multiple clusters. Clusters are reported as 'cluster mass [segment range]'. CC – congenital cataract reversal individuals; CB – Permanently congenitally blind individuals; SC – Normally sighted control individuals; FA – Fractional anisotropy; MD – Mean diffusivity; RD – Radial diffusivity; AD – Axial diffusivity.

Inferior Fronto-Occipital Fasciculus

Compared with SC, CB individuals had decreased FA, and increased MD and RD (figures 4B & 5B, table 4), while CC subjects had increased MD, RD and AD (figures 4A & 5A, table 4). These differences mostly presented bilaterally and appeared to exhibit spatial similarity across hemispheres. Comparing CC and CB groups, CC individuals had significantly higher FA, lower MD and RD in the right hemisphere, but no differences in AD (figures 4C & 5C, table 4). Clusters found in CC vs SC and CC vs CB comparisons seemed to have overlap with clusters seen in CB vs SC comparisons, but not with each other.

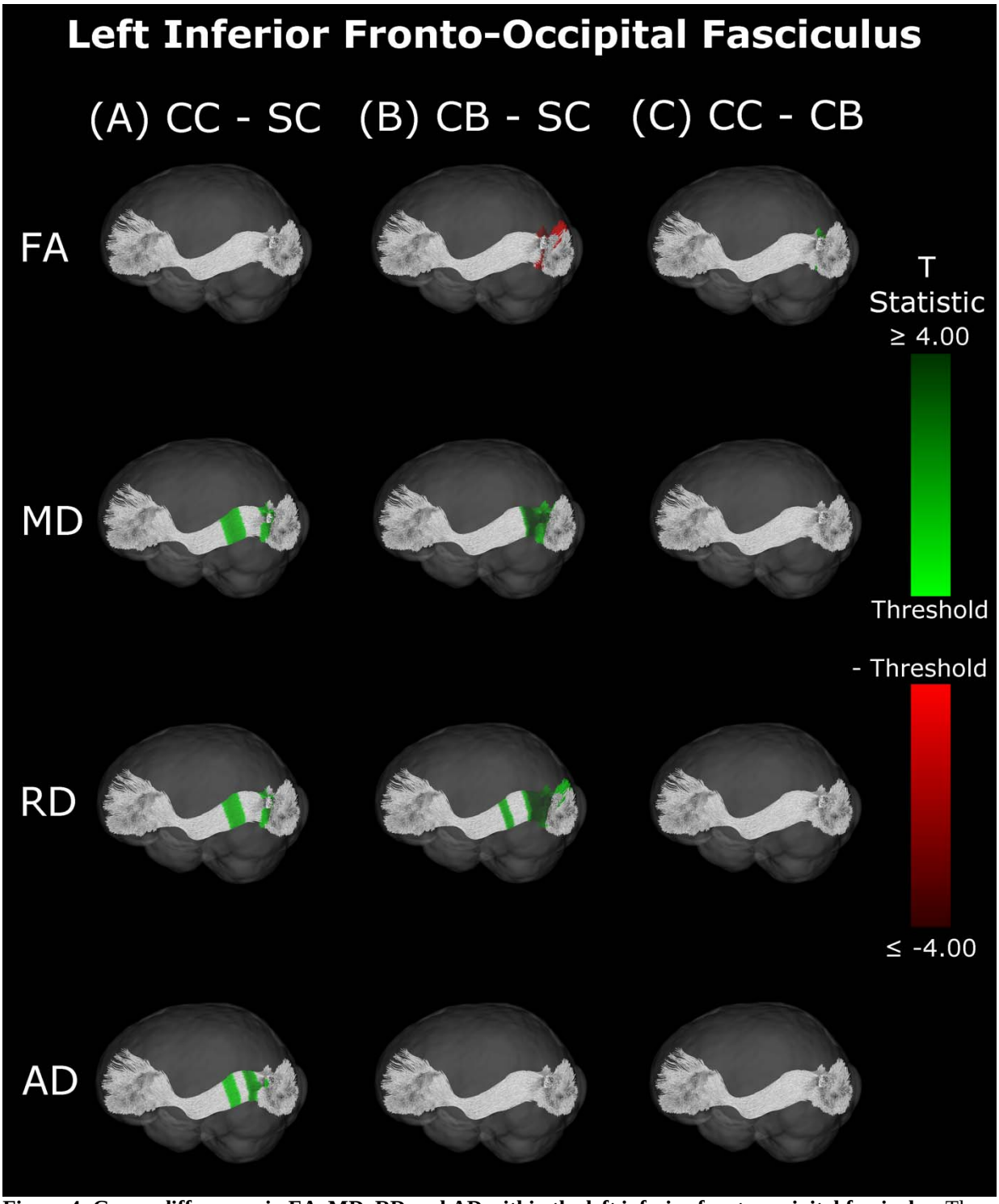

Figure 4: Group differences in FA, MD, RD and AD within the left inferior fronto-occipital fasciculus. The transposed segmentation of the left inferior fronto-occipital fasciculus is coloured according to the spatial location of clusters of significant differences between A) CC and SC individuals, B) CB and SC individuals, and C) CC and CB individuals. Segments coloured green indicate that the metric is higher in the first group than the second, while red segments specify the opposite. The shade of colour encodes the degree of difference, with light shades representing near-threshold T-statistics (2.032; 2.145; 2.056), and darker shades reflecting larger T-statistics. CC – congenital cataract reversal individuals; CB – Permanently congenitally blind individuals; SC – Normally sighted control individuals; FA – Fractional anisotropy; MD – Mean diffusivity; RD – Radial diffusivity; AD – Axial diffusivity.

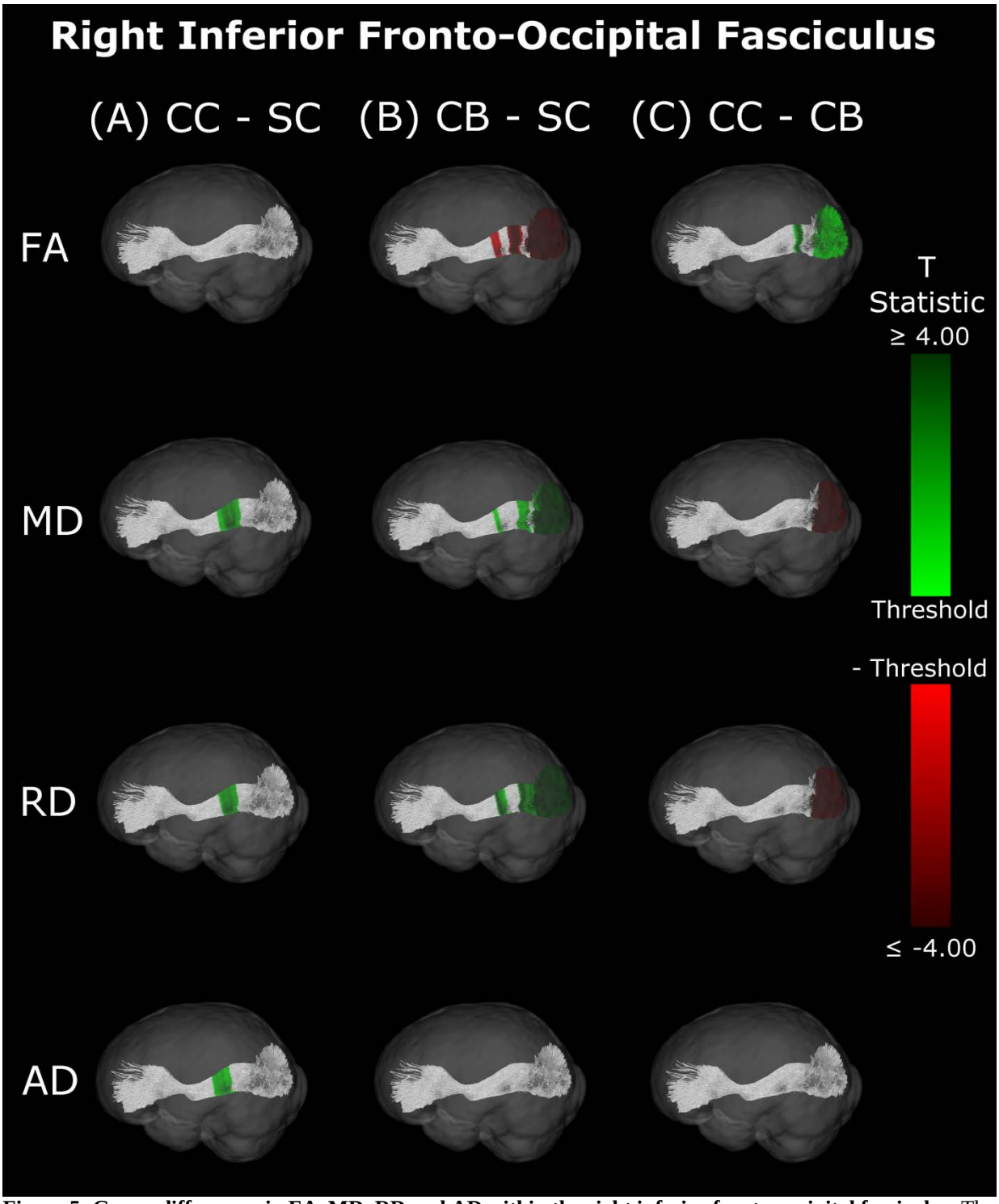

Figure 5: Group differences in FA, MD, RD and AD within the right inferior fronto-occipital fasciculus. The transposed segmentation of the right inferior fronto-occipital fasciculus is coloured according to the spatial location of clusters of significant differences between A) CC and SC individuals, B) CB and SC individuals, and C) CC and CB individuals. Segments coloured green indicate that the metric is higher in the first group than the second, while red segments specify the opposite. The shade of colour encodes the degree of difference, with light shades representing near-threshold T-statistics (2.032; 2.145; 2.056), and darker shades reflecting larger T-statistics. CC – congenital cataract reversal individuals; CB – Permanently congenitally blind individuals; SC – Normally sighted

control individuals; FA – Fractional anisotropy; MD – Mean diffusivity; RD – Radial diffusivity; AD – Axial diffusivity.

Table 4. Cluster masses and segment ranges for the left and right inferior fronto-occipital fasciculi, by group comparison, hemisphere, and metric.

Inferior Fronto-Occipital Fasciculus						
	CC vs SC		CB vs SC		CC vs CB	
Metric	Left	Right	Left	Right	Left	Right
FA			33.93 [86-97]	17.86 [59-65] 37.76 [72-81] 62.53 [86-98]	10.75 [89-92]	18.04 [75-80] 16.32 [93-98]
MD	29.1 [60-71] 15.83 [82-88]	49 [55-72]	57.69 [75-93]	9.12 [59-62] 22.45 [77-85] 31.67 [89-98]		15.76 [95-98]
RD	23.9 [62-71] 13.39 [83-88]	38.13 [59-72]	13.16 [61-65] 80.84 [75-97]	27.52 [58-66] 93.92 [75-98]		18.72 [94-98]
AD	15.38 [63-69] 15.38 [75-80]	36.5 [54-68]				

Table note: Each entry refers to a cluster of significantly different segments found in the left or right optic inferior fronto-occipital fasciculus, organized by group comparison, hemisphere and tensor metric. Multiple entries refer to multiple clusters. Clusters are reported as 'cluster mass [segment range]'. CC – congenital cataract reversal individuals; CB – Permanently congenitally blind individuals; SC – Normally sighted control individuals; FA – Fractional anisotropy; MD – Mean diffusivity; RD – Radial diffusivity; AD – Axial diffusivity.

Inferior Longitudinal Fasciculus

The CB group showed decreased FA, and increased MD and RD compared to the SC group (figure 6B & 7B, table 5). Similar patterns were observed, as well as lower AD, when comparing CB to CC individuals (figure 6C & 7C, table 5). Most of these differences existed bilaterally and displayed spatial similarity across hemispheres. In contrast, CC individuals exhibited very few differences compared to SC subjects; AD in the left hemisphere was higher (figure 6A, table 5), while FA in the right hemisphere was decreased (figure 7A, table 5). The latter of these differences showed overlap with clusters in the corresponding CB vs SC comparison of FA, while nearly all clusters in CC vs CB comparisons appeared to have spatial overlap with CB vs SC clusters.

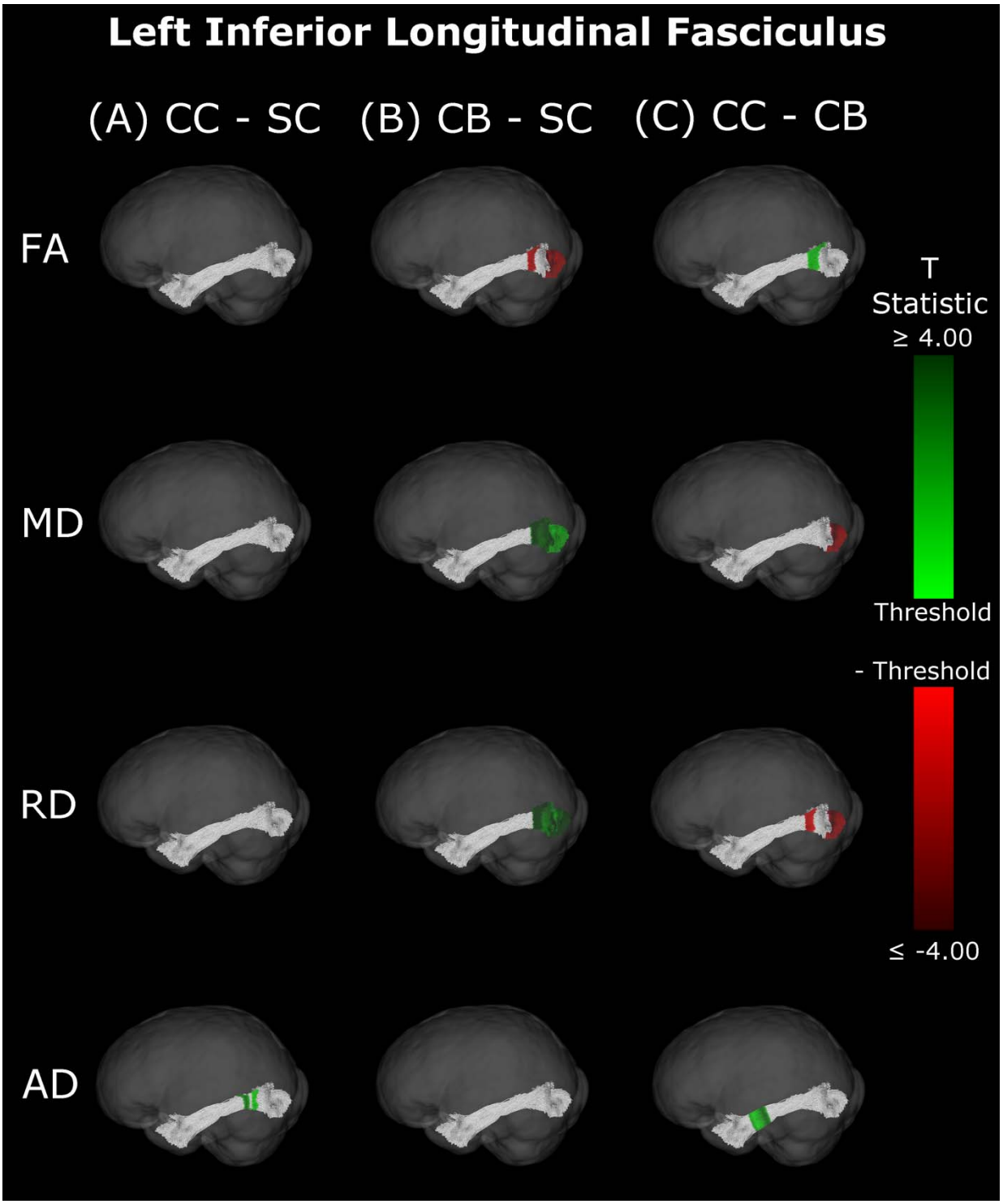

Figure 6: Group differences in FA, MD, RD and AD within the left inferior longitudinal fasciculus. The transposed segmentation of the left inferior longitudinal fasciculus is coloured according to the spatial location of clusters of significant differences between A) CC and SC individuals, B) CB and SC individuals, and C) CC and CB individuals. Segments coloured green indicate that the metric is higher in the first group than the second, while red segments specify the opposite. The shade of colour encodes the degree of difference, with light shades representing near-threshold T-statistics (2.032; 2.145; 2.056), and darker shades reflecting larger T-statistics. CC – congenital cataract reversal individuals; CB – Permanently congenitally blind individuals; SC – Normally sighted control individuals; FA – Fractional anisotropy; MD – Mean diffusivity; RD – Radial diffusivity; AD – Axial diffusivity.

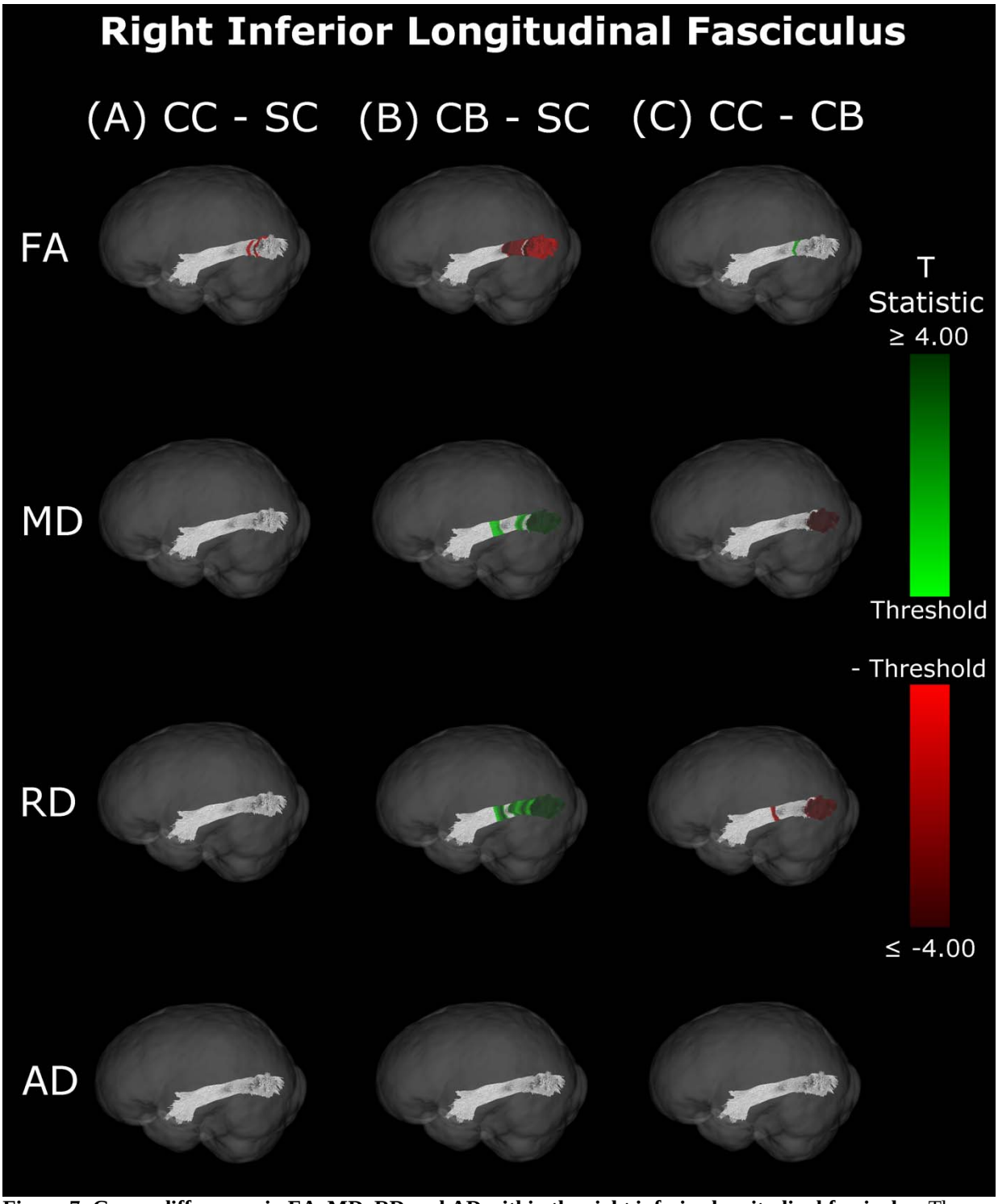

Figure 7: Group differences in FA, MD, RD and AD within the right inferior longitudinal fasciculus. The transposed segmentation of the right inferior longitudinal fasciculus is coloured according to the spatial location of clusters of significant differences between A) CC and SC individuals, B) CB and SC individuals, and C) CC and CB individuals. Segments coloured green indicate that the metric is higher in the first group than the second, while red segments specify the opposite. The shade of colour encodes the degree of difference, with light shades representing near-threshold T-statistics (2.032; 2.145; 2.056), and darker shades reflecting larger T-statistics. CC – congenital cataract reversal individuals; CB – Permanently congenitally blind individuals; SC – Normally sighted control individuals; FA – Fractional anisotropy; MD – Mean diffusivity; RD – Radial diffusivity; AD – Axial diffusivity.

Table 5. Cluster masses and segment ranges for the left and right inferior longitudinal fasciculi, by group comparison, hemisphere, and metric.

Inferior Longitudinal Fasciculus						
	CC vs SC		CB vs SC		CC vs CB	
Metric	Left	Right	Left	Right	Left	Right
FA		8.47 [80-83] 13.33 [90-95]	15.48 [71-76] 43.81 [85-98]	80.49 [61-84] 41.97 [86-98]	20.81 [69-77]	9.91 [73-76]
MD			96.92 [70-98]	26.1 [43-53] 23.87 [74-82] 44.01 [87-98]	24.64 [91-98]	19.06 [94-98]
RD			110.71 [70-98]	36.43 [43-54] 130.5 [60-98]	15.99 [69-75] 27.04 [90-98]	13.87 [49-53] 14.64 [94-98]
AD	14.22 [63-67] 8.5 [70-73]				37.03 [23-36]	

Table note: Each entry refers to a cluster of significantly different segments found in the left or right inferior longitudinal fasciculus, organized by group comparison, hemisphere and tensor metric. Multiple entries refer to multiple clusters. Clusters are reported as 'cluster mass [segment range]'. CC – congenital cataract reversal individuals; CB – Permanently congenitally blind individuals; SC – Normally sighted control individuals; FA – Fractional anisotropy; MD – Mean diffusivity; RD – Radial diffusivity; AD – Axial diffusivity.

Correlations with behaviour and demographics

An exploratory analysis was performed to test whether mean metric values in the visual tracts of CC individuals were correlated with visual acuity, age at surgery, or time since surgery. For each metric, the mean of all 98 segments of each tract was calculated and was then correlated to visual acuity, age at surgery, and time since surgery, while correcting for the effect of age. Only one correlation was found to be significant (AD values in the left SLF were significantly correlated with time since surgery ($p=0.037$)), but this did not survive multiple comparisons correction (Spearman's rho values are reported in supplementary tables 5, 6 and 7). Additional along-the-tract correlation analyses of the optic radiations also failed to detect significant correlations which survived statistical thresholding (not shown).

Summary

Overall, group differences in DTI metrics were almost exclusively found in visual tracts. When these differences existed bilaterally, they displayed spatial similarity across hemispheres. Compared to SC, CC individuals seemed to have increased MD, RD and AD in most visual tracts, but few differences in FA. Conversely, CB individuals featured extensively decreased FA relative to SC subjects, as well as increased MD and RD. Furthermore, these differences were relatively greater than those of CC vs SC participants, as evidenced by larger cluster masses. Accordingly, a direct comparison between CC and CB individuals indicated significantly increased FA, and significantly decreased MD and RD in the CC group. Moreover, group differences between CC and SC individuals appeared to have considerable spatial overlap with the 'large' clusters seen in CB vs SC comparisons, particularly near the occipital terminals of tracts.

Discussion

Congenital blindness has been demonstrated to be associated with white matter microstructure alterations in visual tracts [11]. Yet, it was unknown whether these changes are permanent or would recover if sight was restored. To test for white matter changes as a consequence of sight restoration after congenital blindness and, we acquired diffusion tensor image scans in congenitally blind individuals with restored sight due to cataract reversal surgery, permanently congenitally blind humans, individuals with reversed developmental (late-onset childhood) cataracts and age and sex matched normally sighted controls.

Results replicated previous findings in permanently congenitally blind individuals (CB group in the present study), who showed considerable degradation of white matter microstructure in

visual tracts relative to SC subjects [10,11,41,42,46]. CC individuals exhibited some impairments in white matter microstructure as well, despite having underwent sight-restoring surgery. However, DTI metrics in the CC group additionally suggested a considerable degree of recovery compared to CB individuals.

Congenital blindness and white matter impairment

Overall, DTI metrics indicated that white matter is impaired in CB relative to SC subjects. The presentation of increased MD points towards an overall increase in diffusivity within visual tracts. The concurrent finding of increased RD, with less support for widespread changes in AD, suggests that the increase in overall diffusivity is likely driven by a lower degree of myelination [32,33]. This is supported by the additionally observed decrease in FA, which indicates a decline in the ability of a tract to constrain diffusion to the primary direction. While no study to date has histologically assessed myelination in a permanently congenitally blind human population, some neuroimaging studies have speculated that there may be lower myelination in visual cortex in this population [25,58,59].

In the present study, differences in DTI metrics were observed for the optic radiation, splenium, IFOF and ILF, but not the SLF. While the literature on permanent congenital blindness is widely varied, a large number of our findings are in line with results from previous studies. Many of these previous studies have demonstrated degradation of the optic radiation via decreased FA, increased MD or RD [10,35–39,41–44], reinforcing the widespread bilateral changes reported in the present study. In the IFOF and ILF, support from the literature is less extensive, but still present; some studies have found decreased FA in the IFOF and ILF, but not the SLF [38,42,46], reinforcing

the current results, including the null finding in the SLF. For the splenium, some studies are consistent with the present finding of alterations [38,44], while others did not observe differences between CB and SC individuals [42,45].

Persisting white matter impairment in congenital cataract reversal individuals

Importantly, while some differences seen in CC individuals relative to SC individuals mirrored those observed between CB and SC participants (although to a much lower extent), we observed qualitative differences as well. Similar to CB participants, the observed increase in MD indicates that there was an elevated level of overall diffusivity within visual tracts of CC individuals compared to the SC group. However, elevated MD was accompanied by increases in both RD and AD for the CC group, suggesting that differences were not due to a single mechanism. The absence of extensive changes in FA for CC individuals supports the idea that the overall shape of the diffusion tensor was unchanged, supported by the coinciding increase in RD and AD.

While higher RD intuitively suggests a lower degree of myelination [32,33], AD is typically thought of as an indicator of axonal integrity [33,34]. Non-human animal work has reported that sensory deprivation induced changes in myelin were not accompanied by changes to the axons, which remained intact [60]. Although our data do not allow us to draw final conclusions about the underlying mechanisms behind higher AD in the CC group compared to the SC group, given that lower AD has previously been associated with axonal pruning [61], we speculate that the present results may be due to reduced axonal pruning during early development or axon growth after sight restoration.

Given that only one previous study [47] has explored white matter microstructure in congenital cataract reversal individuals, it seems crucial to compare both studies' results where possible; Pedersini et al. (2023) [47] explored mean FA and MD, but not RD and AD in CC individuals. In CC vs SC comparisons, our findings of increased MD and relatively unchanged FA are consistent with the cross-sectional findings of Pedersini et al. (2023) [47]. However, while we found group differences in MD to be relatively limited to the optic radiation, splenium and IFOF, these authors reported a main effect of group on MD for *all* tracts, including the non-visual tracks. This surprising finding from Pedersini et al. (2023) [47] might be related to the absence of their own control group; these authors did not scan controls, but rather extracted control data from the Human Connectome Project - Development sample, which involved different acquisition parameters and did not include subjects from the same country (India).

White matter recovery after sight restoration in congenital cataract reversal individuals

Compared directly to CB subjects, increased FA and decreased MD and RD seem to point towards some degree of recovery in CC individuals. Elevated FA values indicate that tracts are better able to constrain diffusion to the longitudinal axis. However, the reduction in overall diffusivity suggested by lower MD in CC individuals would indicate that group differences in FA are not purely driven by an increase in diffusion along this axis, but rather a reduction in the amount of diffusion in other axes as well. This hypothesis is supported by the concurrent observation of decreased RD. Overall, this pattern of results for the comparison of CC and CB participants would suggest that white matter recovery after sight restoration is largely driven by

an increase in myelination [32,33] of visual tracts, consistent with activity regulated mechanisms of myelin plasticity available throughout life [62].

Remarkably, lower MD, RD and AD values were consistent across hemispheres in CC compared to CB individuals in segments where the optic radiation connects with the primary visual cortex. In contrast, no differences between the CC and SC group were observed here. These results suggest considerable recovery of thalamo-cortical connectivity in CC individuals. Pedersini et al. (2023) [47] were unable to identify any longitudinal changes in the optic radiation, possibly due to using average values across the complete tract.

The pattern of results observed in the comparison between CC vs. CB individuals for the optic radiations was also observed for the IFOF and ILF, but not for the splenium or SLF, which is in partial agreement with the longitudinal findings of Pedersini et al. (2023) [47]. Specifically, while these authors found longitudinal increases in FA for the ILF and IFOF, they additionally observed differences in the SLF and reductions in MD of the splenium, which we did not find when comparing CC individuals to the CB group.

Our findings in the ILF are not only consistent with those of Pedersini et al. (2023) [47], but are quite compelling in their own right. While we found large bilateral group differences for FA, MD and RD between CB and SC subjects, which was consistent with previous studies [10,38,42,46], in CC vs SC comparisons only FA was reduced in the right ILF and only AD was increased in the left ILF. The ILF is the major white matter tract of the ventral visual stream. A recent fMRI study has identified an impressive recovery of visual categorical representations in CC

individuals' in the ventral occipito-temporal cortex compatible with the extensive white matter recovery suggested by the CC vs. CB comparison of the present study. Consistent with electrophysiological results [18,63], Rączy et al. (2025) [64] has recently reported largely reduced face-selectivity in CC individuals but largely unchanged selectivity for scenes. Face processing typically features a right hemispheric dominance. Thus, the lower recovery of FA in the right ILF might mirror the functional changes and observed impairments in face processing in CC individuals, while the larger pattern of ILF recovery is consistent with the high recovery of object recognition [17,19,65].

Spatial distribution of group differences indicates some specificity

As a particular strength of the along-the-tract approach, our results showed an impressive pattern of spatial specificity. In the comparison between CB vs SC individuals, while significant clusters can be found throughout the tract, they are very prominently located at or near the occipital terminals of all tracts. Crucially, most significant group differences between CC and CB individuals were also found near the occipital terminals, and thus overlapped with differences between CB and SC individuals. In contrast, while CC vs SC clusters did not appear in occipital areas for any tract, they did overlap with a subset of CB vs SC clusters in other locations. These results might suggest a high capacity for recovery at the occipital terminals of several visual tracts, as well as persisting impairments related to temporary congenital blindness.

Experience-dependent myelination accounts for both impairment and recovery

Traditionally, myelin has been considered to be a rather static structure, that follows strict developmental trajectories and remains stable throughout the lifespan [66]. Prior studies have defined typical developmental trajectories for various regions of the brain, suggesting that myelination begins in the cerebellum, pons and internal capsule, then spreads to the splenium and optic radiation (3-4 months), the occipital and parietal cortices (4-6 months), and temporal and frontal cortices (6-8 months) [67]. In the optic tract, myelin can be seen (ex vivo) at term, and increases considerably in the first two years of life, then slower afterwards [68]. More recent studies have uncovered extraordinary adult myelin plasticity, providing an increasing amount of support for an activity-dependent, and thereby experience-dependent, myelination [43,66,69,70]. Neural activity is not strictly necessary for myelination to emerge in the first place during development [66]. However, studies have indicated that neuron activity can have a vast impact on myelination [71–73]. In addition to *de novo* myelination of 'naked' axons [74], or the retraction of existing sheaths, myelination can additionally be remodelled through mechanisms that modulate myelin sheath length, myelin thickness, and the nodes of Ranvier [62,75–77].

Neurons can synapse directly onto oligodendrocyte precursor cells [78], so a lack of visual activity may reduce the production and maturation of the glial cells driving myelination in the central nervous system. A reduction in oligodendrogenesis could coincide with an increase in cortical excitability since some of the major inhibitory interneurons (e.g. parvalbumin positive GABAergic interneurons) are typically heavily myelinated [60]. A higher excitatory-inhibitory ratio in occipital cortex is a common finding in congenital blindness [29,79,80]. This ratio shows partial recovery in CC compared to CB individuals [18,29], but future studies are needed to explore a potential link to myelin plasticity.

Structural changes following sight restoration seemingly rely on mechanisms of myelin plasticity, like *de novo* myelination or myelin remodelling [62,74–77], via oligodendrogenesis and the proliferation of new oligodendrocyte precursor cells [81]. However, studies have suggested that differences between mechanisms of developmental myelination and later white matter plasticity exist [66,81]. Thus, we speculate that while the extensive recovery we found (compared to the CB group) might be due to mechanisms of later myelin plasticity, the persisting impairments we observed in the CC group (compared to the SC group) might indicate that adult myelin plasticity partially builds on early white matter development. While myelination can considerably increase neuronal efficiency [82], there is a metabolic cost of development and maintenance. As such, a cost-efficient approach would not include indiscriminate myelination of all axons, but could instead partially rely on activity to determine the most important connections to myelinate, or which sheaths to maintain or improve over the complete life span.

Limitations and future directions

Our study has a number of limitations to consider. The CB group can, at most, be an approximation of pre-surgery CC participants. While CB participants were all born blind, the causes of blindness were variable and often related to the retina. Two CB participants were additionally unable to perceive light. A longitudinal approach similar to that of Pedersini et al. (2023) [47] would allow a more direct tracking of white matter plasticity following sight restoration. Secondly, while our sample was quite large considering the exceeding rarity of the CC population, sample size is almost always a limitation in research with rare clinical

populations. Regarding the lack of correlations with variables of interest (visual acuity, age at surgery, time since surgery), we speculate that visual acuity might not be a sensitive metric for white matter changes, that persisting impairments in CC individuals may have emerged early in brain development, and that most of the recovery (observed here as null effects compared to SC individuals) occurred shortly after sight recovery. Lastly, the neurobiological interpretations of the present data rely on biomarkers that are not fully specific. While RD and AD are closely related to myelin [32,33] and axonal integrity [33,34] respectively, they can be influenced by other factors as well. Thus, nailing down the precise mechanisms underlying the observed white matter changes is not possible with DTI data [31,62]

Conclusion

Ultimately, using a granular along-the-tract approach, we replicated the extensive differences between permanently congenitally blind and sighted control participants in the main visual tracts. Additionally, we found some persisting differences between normally sighted controls and congenital cataract reversal individuals, supporting the idea of a sensitive period for white matter microstructure in early visual development. However, differences between congenital cataract reversal individuals and permanently congenitally blind individuals, as well as fewer differences compared to normally sighted controls (which were highly significant for the permanently congenitally blind group) suggest that there is extensive recovery in white matter microstructure. We speculate that the main factors driving our results are related to mechanisms of myelin development and plasticity, which is consistent with the idea that life-long myelin plasticity (see as well Pedersini et al., 2023) [47] may be higher than neuronal structural plasticity (measured via metrics of cortical morphometry [25,27]).

Data Availability

Anonymized subject information, aggregated data and code are available at the following DOI: https://doi.org/ 10.25592/uhhfdm.17938. Further data can be made available upon reasonable request to the corresponding author from any qualified investigator.

CRediT Author Contributions

JDH: Conceptualization, Methodology, Formal Analysis, Visualization, Writing – Original Draft. **CH:** Methodology, Data Curation, Writing – Review & Editing, Supervision. **SL:** Resources, Writing – Review & Editing. **RK:** Conceptualization, Resources, Writing – Review & Editing. **BR:** Conceptualization, Resources, Writing – Original Draft, Supervision, Project Administration, Funding Acquisition.

Funding

This study was supported by funding to BR from the German Research Foundation (DFG Ro 2625/10-1), the European Research Council (ERC-2009-AdG 249425-CriticalBrainChanges). JH is funded by the Max Planck School of Cognition.

Competing Interests

Sunitha Lingareddy is the Managing Director of Radiology at Lucid Medical Diagnostics Banjara Hills, Hyderabad, India.

We report no other competing interests.

Acknowledgements

We appreciate the contributions of Maria Guerreiro during study initiation, data collection and curation, and thank Seema Banerjee and Divya Jagadish for help with participant recruitment and data acquisition, as well as Armin Heinecke for an initial data quality check. We are grateful to Kabilan Pitchaimuthu, Prativa Regmi and Idris Shareef for providing clinical details of the participants during the classification process. We thank the technical staff of the Lucid Medical Diagnostics Banjara Hills in Hyderabad in India for technical assistance during collection of MRI data. We are grateful to D. Balasubramanian from the LV Prasad Eye Institute for supporting the research.

References

1. Gabard-Durnam L, McLaughlin KA. Sensitive periods in human development: charting a course for the future. *Curr Opin Behav Sci*. 2020;36:120-128. doi:10.1016/j.cobeha.2020.09.003

2. Reh RK, Dias BG, Nelson CA, et al. Critical period regulation across multiple timescales. *Proc Natl Acad Sci*. 2020;117(38):23242-23251. doi:10.1073/pnas.1820836117

3. Knudsen EI. Sensitive Periods in the Development of the Brain and Behavior. *J Cogn Neurosci*. 2004;16(8):1412-1425. doi:10.1162/0898929042304796

4. Hubel DH, Wiesel TN. The period of susceptibility to the physiological effects of unilateral eye closure in kittens. *J Physiol*. 1970;206(2):419-436. doi:10.1113/jphysiol.1970.sp009022

5. Harwerth RS, Smith EL, Duncan GC, Crawford MLJ, von Noorden GK. Multiple Sensitive Periods in the Development of the Primate Visual System. *Science*. 1986;232(4747):235-238. doi:10.1126/science.3952507

6. Levelt CN, Hübener M. Critical-Period Plasticity in the Visual Cortex. *Annu Rev Neurosci*. 2012;35(Volume 35, 2012):309-330. doi:10.1146/annurev-neuro-061010-113813

7. Lewis TL, Maurer D. Multiple sensitive periods in human visual development: Evidence from visually deprived children. *Dev Psychobiol*. 2005;46(3):163-183. doi:10.1002/dev.20055

8. Mitchell DE, Maurer D. Critical Periods in Vision Revisited. *Annu Rev Vis Sci*. 2022;8(Volume 8, 2022):291-321. doi:10.1146/annurev-vision-090721-110411

9. Röder B, Kekunnaya R, Guerreiro MJS. Neural mechanisms of visual sensitive periods in humans. *Neurosci Biobehav Rev*. 2021;120:86-99. doi:10.1016/j.neubiorev.2020.10.030

10. Bridge H, Coullon GSL, Morjaria R, et al. The Effect of Congenital and Acquired Bilateral Anophthalmia on Brain Structure. *Neuro-Ophthalmol*. 2021;45(2):75-86.

11. Paré S, Bleau M, Dricot L, Ptito M, Kupers R. Brain structural changes in blindness: a systematic review and an anatomical likelihood estimation (ALE) meta-analysis. *Neurosci Biobehav Rev*. 2023;150:105165. doi:10.1016/j.neubiorev.2023.105165

12. Renier L, De Volder AG, Rauschecker JP. Cortical plasticity and preserved function in early blindness. *Neurosci Biobehav Rev*. 2014;41:53-63. doi:10.1016/j.neubiorev.2013.01.025

13. Röder B, Kekunnaya R. Effects of Early Visual Deprivation. In: *Oxford Research Encyclopedia of Psychology*. 2022. doi:10.1093/acrefore/9780190236557.013.839

14. Birch EE, Cheng C, Stager DR, Weakley DR, Stager DR. The critical period for surgical treatment of dense congenital bilateral cataracts. *J Am Assoc Pediatr Ophthalmol Strabismus JAAPOS*. 2009;13(1):67-71. doi:10.1016/j.jaapos.2008.07.010

15. Khanna RC, Foster A, Krishnaiah S, Mehta MK, Gogate PM. Visual outcomes of bilateral congenital and developmental cataracts in young children in south India and causes of poor outcome. *Indian J Ophthalmol*. 2013;61(2):65. doi:10.4103/0301-4738.107194

16. Rajendran SS, Bottari D, Shareef I, et al. Biological Action Identification Does Not Require Early Visual Input for Development. *eNeuro*. 2020;7(5). doi:10.1523/ENEURO.0534-19.2020

17. Le Grand R, Mondloch CJ, Maurer D, Brent HP. Early visual experience and face processing. *Nature*. 2001;410(6831):890-890. doi:10.1038/35073749

18. Ossandón JP, Rossion B, Dormal G, Kekunnaya R, Röder B. Impaired rapid neural face categorization after reversing long-lasting congenital blindness. *Cortex*. 2025;187:124-139. doi:10.1016/j.cortex.2025.04.007

19. Putzar L, Hötting K, Röder B. Early visual deprivation affects the development of face recognition and of audio-visual speech perception. *Restor Neurol Neurosci*. 2010;28(2):251-257. doi:10.3233/RNN-2010-0526

20. Bottari D, Troje NF, Ley P, Hense M, Kekunnaya R, Röder B. The neural development of the biological motion processing system does not rely on early visual input. *Cortex*. 2015;71:359-367. doi:10.1016/j.cortex.2015.07.029

21. Gandhi TK, Ganesh S, Sinha P. Improvement in Spatial Imagery Following Sight Onset Late in Childhood. *Psychol Sci*. Published online January 9, 2014. doi:10.1177/0956797613513906

22. Hadad BS, Maurer D, Lewis TL. Sparing of sensitivity to biological motion but not of global motion after early visual deprivation. *Dev Sci*. 2012;15(4):474-481. doi:10.1111/j.1467-7687.2012.01145.x

23. Pitchaimuthu K, Sourav S, Bottari D, et al. Color vision in sight recovery individuals. *Restor Neurol Neurosci*. 2019;37(6):583-590. doi:10.3233/RNN-190928

24. Röder B, Kekunnaya R. Visual experience dependent plasticity in humans. *Curr Opin Neurobiol*. 2021;67:155-162. doi:10.1016/j.conb.2020.11.011

25. Hölig C, Guerreiro MJS, Lingareddy S, Kekunnaya R, Röder B. Sight restoration in congenitally blind humans does not restore visual brain structure. *Cereb Cortex*. 2023;33(5):2152-2161. doi:10.1093/cercor/bhac197

26. Feng Y, Collignon O, Maurer D, Yao K, Gao X. Brief Postnatal Visual Deprivation Triggers Long-Lasting Interactive Structural and Functional Reorganization of the Human Cortex. *Front Med*. 2021;8. doi:10.3389/fmed.2021.752021

27. Guerreiro MJS, Erfort MV, Henssler J, Putzar L, Röder B. Increased visual cortical thickness in sight-recovery individuals. *Hum Brain Mapp*. 2015;36(12):5265-5274. doi:10.1002/hbm.23009

28. Heitmann C, Zhan M, Linke M, et al. Early visual experience refines the retinotopic organization within and across visual cortical regions. *Curr Biol*. 2023;33(22):4950-4959.e4. doi:10.1016/j.cub.2023.10.010

29. Rączy K, Hölig C, Guerreiro MJS, Lingareddy S, Kekunnaya R, Röder B. Typical resting-state activity of the brain requires visual input during an early sensitive period. *Brain Commun*. 2022;4(4):fcac146. doi:10.1093/braincomms/fcac146

30. Pant R, Pitchaimuthu K, Ossandón J, et al. Altered visual cortex excitatory/inhibitory ratio following transient congenital visual deprivation in humans. *eLife*. 2025;13. doi:10.7554/eLife.98143.2

31. Walhovd KB, Johansen-Berg H, Káradóttir RT. Unraveling the secrets of white matter – Bridging the gap between cellular, animal and human imaging studies. *Neuroscience*. 2014;276:2-13. doi:10.1016/j.neuroscience.2014.06.058

32. Alexander AL, Lee JE, Lazar M, Field AS. Diffusion Tensor Imaging of the Brain. *Neurotherapeutics*. 2007;4(3):316-329. doi:10.1016/j.nurt.2007.05.011

33. Song SK, Sun SW, Ramsbottom MJ, Chang C, Russell J, Cross AH. Dysmyelination Revealed through MRI as Increased Radial (but Unchanged Axial) Diffusion of Water. *NeuroImage*. 2002;17(3):1429-1436. doi:10.1006/nimg.2002.1267

34. Song SK, Sun SW, Ju WK, Lin SJ, Cross AH, Neufeld AH. Diffusion tensor imaging detects and differentiates axon and myelin degeneration in mouse optic nerve after retinal ischemia. *NeuroImage*. 2003;20(3):1714-1722. doi:10.1016/j.neuroimage.2003.07.005

35. Zhang Y, Wan S, Ge J, Zhang X. Diffusion tensor imaging reveals normal geniculocalcarine-tract integrity in acquired blindness. *Brain Res*. 2012;1458:34-39. doi:10.1016/j.brainres.2012.04.012

36. Wang D, Qin W, Liu Y, Zhang Y, Jiang T, Yu C. Altered White Matter Integrity in the Congenital and Late Blind People. *Neural Plast*. 2013;2013(1):128236. doi:10.1155/2013/128236

37. Shu N, Li J, Li K, Yu C, Jiang T. Abnormal diffusion of cerebral white matter in early blindness. *Hum Brain Mapp*. 2009;30(1):220-227. doi:10.1002/hbm.20507

38. Reislev NL, Dyrby TB, Siebner HR, Kupers R, Ptito M. Simultaneous Assessment of White Matter Changes in Microstructure and Connectedness in the Blind Brain. *Neural Plast*. 2016;2016(1):6029241. doi:10.1155/2016/6029241

39. Hofstetter S, Sabbah N, Mohand-Saïd S, et al. The development of white matter structural changes during the process of deterioration of the visual field. *Sci Rep*. 2019;9(1):2085. doi:10.1038/s41598-018-38430-5

40. Dietrich S, Hertrich I, Kumar V, Ackermann H. Experience-Related Structural Changes of Degenerated Occipital White Matter in Late-Blind Humans – A Diffusion Tensor Imaging Study. *PLOS ONE*. 2015;10(4):e0122863. doi:10.1371/journal.pone.0122863

41. Ankeeta A, Kumaran SS, Saxena R, Jagannathan NR. Structural and white matter changes associated with duration of Braille education in early and late blind children. *Vis Neurosci*. 2021;38:E011. doi:10.1017/S0952523821000080

42. Bridge H, Cowey A, Ragge N, Watkins K. Imaging studies in congenital anophthalmia reveal preservation of brain architecture in 'visual' cortex. *Brain*. 2009;132(12):3467-3480. doi:10.1093/brain/awp279

43. Anurova I, Carlson S, Rauschecker JP. Overlapping Anatomical Networks Convey Cross-Modal Suppression in the Sighted and Coactivation of "Visual" and Auditory Cortex in the Blind. *Cereb Cortex*. 2019;29(11):4863-4876. doi:10.1093/cercor/bhz021

44. Shimony JS, Burton H, Epstein AA, McLaren DG, Sun SW, Snyder AZ. Diffusion Tensor Imaging Reveals White Matter Reorganization in Early Blind Humans. *Cereb Cortex N Y N 1991*. 2006;16(11):1653-1661. doi:10.1093/cercor/bhj102

45. Bock AS, Saenz M, Tungaraza R, Boynton GM, Bridge H, Fine I. Visual callosal topography in the absence of retinal input. *NeuroImage*. 2013;81:325-334. doi:10.1016/j.neuroimage.2013.05.038

46. Reislev NL, Kupers R, Siebner HR, Ptito M, Dyrby TB. Blindness alters the microstructure of the ventral but not the dorsal visual stream. *Brain Struct Funct*. 2016;221(6):2891-2903. doi:10.1007/s00429-015-1078-8

47. Pedersini CA, Miller NP, Gandhi TK, et al. White matter plasticity following cataract surgery in congenitally blind patients. *Proc Natl Acad Sci*. 2023;120(19):e2207025120. doi:10.1073/pnas.2207025120

48. Yeatman JD, Dougherty RF, Myall NJ, Wandell BA, Feldman HM. Tract Profiles of White Matter Properties: Automating Fiber-Tract Quantification. *PLOS ONE*. 2012;7(11):e49790. doi:10.1371/journal.pone.0049790

49. Lewis TL, Maurer D, Brent HP. Development of grating acuity in children treated for unilateral or bilateral congenital cataract. *Invest Ophthalmol Vis Sci*. 1995;36(10):2080-2095.

50. Kalia A, Lesmes LA, Dorr M, et al. Development of pattern vision following early and extended blindness. *Proc Natl Acad Sci*. 2014;111(5):2035-2039. doi:10.1073/pnas.1311041111

51. Tournier JD, Smith R, Raffelt D, et al. MRtrix3: A fast, flexible and open software framework for medical image processing and visualisation. *NeuroImage*. 2019;202:116137. doi:10.1016/j.neuroimage.2019.116137

52. Schilling KG, Blaber J, Huo Y, et al. Synthesized b0 for diffusion distortion correction (Synb0-DisCo). *Magn Reson Imaging*. 2019;64:62-70. doi:10.1016/j.mri.2019.05.008

53. Schilling KG, Blaber J, Hansen C, et al. Distortion correction of diffusion weighted MRI without reverse phase-encoding scans or field-maps. *PLOS ONE*. 2020;15(7):e0236418. doi:10.1371/journal.pone.0236418

54. Wasserthal J, Neher P, Maier-Hein KH. TractSeg - Fast and accurate white matter tract segmentation. *NeuroImage*. 2018;183:239-253. doi:10.1016/j.neuroimage.2018.07.070

55. Naidich TP, Krayenbühl N, Kollias S, Bou-Haidar P, Bluestone AY, Carpenter DM. CHAPTER 12 - White Matter. In: Naidich TP, Castillo M, Cha S, Smirniotopoulos JG, eds. *Imaging of the Brain*. W.B. Saunders; 2013:205-244. doi:10.1016/B978-1-4160-5009-4.50020-0

56. Wasserthal J, Maier-Hein KH, Neher PF, et al. Multiparametric mapping of white matter microstructure in catatonia. *Neuropsychopharmacology*. 2020;45(10):1750-1757. doi:10.1038/s41386-020-0691-2

57. Chandio BQ, Risacher SL, Pestilli F, et al. Bundle analytics, a computational framework for investigating the shapes and profiles of brain pathways across populations. *Sci Rep*. 2020;10(1):17149. doi:10.1038/s41598-020-74054-4

58. Ptito M, Paré S, Dricot L, Cavaliere C, Tomaiuolo F, Kupers R. A quantitative analysis of the retinofugal projections in congenital and late-onset blindness. *NeuroImage Clin*. 2021;32:102809. doi:10.1016/j.nicl.2021.102809

59. Leporé N, Voss P, Lepore F, et al. Brain structure changes visualized in early- and late-onset blind subjects. *NeuroImage*. 2010;49(1):134-140. doi:10.1016/j.neuroimage.2009.07.048

60. Xin W, Kaneko M, Roth RH, et al. Oligodendrocytes and myelin limit neuronal plasticity in visual cortex. *Nature*. 2024;633(8031):856-863. doi:10.1038/s41586-024-07853-8

61. Gao W, Lin W, Chen Y, et al. Temporal and Spatial Development of Axonal Maturation and Myelination of White Matter in the Developing Brain. *AJNR Am J Neuroradiol*. 2009;30(2):290-296. doi:10.3174/ajnr.A1363

62. Kaller MS, Lazari A, Blanco-Duque C, Sampaio-Baptista C, Johansen-Berg H. Myelin plasticity and behaviour — connecting the dots. *Curr Opin Neurobiol*. 2017;47:86-92. doi:10.1016/j.conb.2017.09.014

63. Röder B, Ley P, Shenoy BH, Kekunnaya R, Bottari D. Sensitive periods for the functional specialization of the neural system for human face processing. *Proc Natl Acad Sci*. 2013;110(42):16760-16765. doi:10.1073/pnas.1309963110

64. Rączy K, Linke M, van den Hurk J, et al. Visual and Auditory Object Representations in Ventral Visual Cortex After Restoring Sight in Humans. *Hum Brain Mapp*. 2025;46(12):e70316. doi:10.1002/hbm.70316

65. Ossandón JP, Zerr P, Shareef I, Kekunnaya R, Röder B. Active Vision in Sight Recovery Individuals with a History of Long-Lasting Congenital Blindness. *eNeuro*. 2022;9(5). doi:10.1523/ENEURO.0051-22.2022

66. Flower G, Vorthmann S, Fulton D, Hamilton NB. Plasticity of Myelination. *Adv Neurobiol*. 2025;43:181-204. doi:10.1007/978-3-031-87919-7_8

67. Deoni SCL, Mercure E, Blasi A, et al. Mapping Infant Brain Myelination with Magnetic Resonance Imaging. *J Neurosci*. 2011;31(2):784-791. doi:10.1523/JNEUROSCI.2106-10.2011

68. Magoon EH, Robb RM. Development of Myelin in Human Optic Nerve and Tract: A Light and Electron Microscopic Study. *Arch Ophthalmol*. 1981;99(4):655-659. doi:10.1001/archopht.1981.03930010655011

69. Fields RD. A new mechanism of nervous system plasticity: activity-dependent myelination. *Nat Rev Neurosci*. 2015;16(12):756-767. doi:10.1038/nrn4023

70. Sampaio-Baptista C, Johansen-Berg H. White Matter Plasticity in the Adult Brain. *Neuron*. 2017;96(6):1239-1251. doi:10.1016/j.neuron.2017.11.026

71. Gibson EM, Purger D, Mount CW, et al. Neuronal Activity Promotes Oligodendrogenesis and Adaptive Myelination in the Mammalian Brain. *Science*. 2014;344(6183):1252304. doi:10.1126/science.1252304

72. Hines JH, Ravanelli AM, Schwindt R, Scott EK, Appel B. Neuronal activity biases axon selection for myelination in vivo. *Nat Neurosci*. 2015;18(5):683-689. doi:10.1038/nn.3992

73. Wake H, Lee PR, Fields RD. Control of Local Protein Synthesis and Initial Events in Myelination by Action Potentials. *Science*. 2011;333(6049):1647-1651. doi:10.1126/science.1206998

74. Wang S, Young KM. White matter plasticity in adulthood. *Neuroscience*. 2014;276:148-160. doi:10.1016/j.neuroscience.2013.10.018

75. Arancibia-Cárcamo IL, Ford MC, Cossell L, Ishida K, Tohyama K, Attwell D. Node of Ranvier length as a potential regulator of myelinated axon conduction speed. Nave KA, ed. *eLife*. 2017;6:e23329. doi:10.7554/eLife.23329

76. Etxeberria A, Hokanson KC, Dao DQ, et al. Dynamic Modulation of Myelination in Response to Visual Stimuli Alters Optic Nerve Conduction Velocity. *J Neurosci*. 2016;36(26):6937-6948. doi:10.1523/JNEUROSCI.0908-16.2016

77. Jeffries MA, Urbanek K, Torres L, Wendell SG, Rubio ME, Fyffe-Maricich SL. ERK1/2 Activation in Preexisting Oligodendrocytes of Adult Mice Drives New Myelin Synthesis and Enhanced CNS Function. *J Neurosci*. 2016;36(35):9186-9200. doi:10.1523/JNEUROSCI.1444-16.2016

78. Moura DMS, Brennan EJ, Brock R, Cocas LA. Neuron to Oligodendrocyte Precursor Cell Synapses: Protagonists in Oligodendrocyte Development and Myelination, and Targets for Therapeutics. *Front Neurosci*. 2022;15. doi:10.3389/fnins.2021.779125

79. Coullon GSL, Emir UE, Fine I, Watkins KE, Bridge H. Neurochemical changes in the pericalcarine cortex in congenital blindness attributable to bilateral anophthalmia. *J Neurophysiol*. 2015;114(3):1725-1733. doi:10.1152/jn.00567.2015

80. Ossandón JP, Stange L, Gudi-Mindermann H, et al. The development of oscillatory and aperiodic resting state activity is linked to a sensitive period in humans. *NeuroImage*. 2023;275:120171. doi:10.1016/j.neuroimage.2023.120171

81. Xin W, Chan JR. Myelin plasticity: sculpting circuits in learning and memory. *Nat Rev Neurosci*. 2020;21(12):682-694. doi:10.1038/s41583-020-00379-8

82. Neishabouri AM, Faisal AA. The metabolic efficiency of myelinated vs unmyelinated axons. *BMC Neurosci*. 2011;12(Suppl 1):P100. doi:10.1186/1471-2202-12-S1-P100

Supplementary Information

Participant information

Supplementary table 1. Congenital cataract reversal participant details (adapted from Hölig et al. (2023) [25])

Participant	Sex	Age (years)	Pre-surgery visual acuity [a]	Age at surgery (y=years, m=months)	Time since surgery (y=years, m=months)	Visual acuity (logMAR) [a]	Additional details
CC1	M	24	N/A	5 m	24 y	0.80	Nystagmus, esotropia
CC2	M	36	N/A	2 y	34 y	0.40	Nystagmus, esotropia
CC3	M	9	CF at 3 m [b]	7 y	3 y	0.80	Nystagmus
CC4	F	6	PL+, PR[+]	4 y	2 y	0.90	Nystagmus
CC5	F	18	CFCF [b]	16 y	3 y	CF at 1 m (1.80 logMAR)	Nystagmus, exotropia, microcornea
CC6	M	32	N/A	6 y	26 y	1.30	Nystagmus
CC7	F	28	CFCF	18 y	10 y	1.10	Nystagmus, esotropia
CC8	M	11	FFL	5 m	11 y	0.90	Nystagmus, esotropia
CC9	M	28	N/A	14 y	15 y	1.00	Nystagmus, esotropia
CC10	M	13	FFL	1 y 3 m	12 y	0.30	Nystagmus, exotropia
CC11	M	32	N/A	29 y 5 m	3 y	1.20[c]	Nystagmus, esotropia
CC12	F	34	1.52 [c]	31 y 4 m	3 y 4 m	1.1	Nystagmus, exotropia
CC13	F	26	N/A	8 m	26 y	0.80	Exotropia [d]
CC14	F	10	FFL	3 y 6 m	7 y	0.40	Nystagmus, exotropia
CC15	F	7	FFL	3 m	7 y	0.80	Nystagmus, esotropia
CC16	F	17	CFCF [b]	10 y 3 m	7 y	1.48[a]	Nystagmus
CC17	F	11	CF at 1 m[e]	10 y 7 m	6 m	1.30	Nystagmus
CC18	M	8	FFL[b]	5 y 4 m	3 y	0.40	Nystagmus, esotropia

CC19	F	18	FFL at 1 m	2 y 1 m	16 y	0.48	Nystagmus, esotropia, microcornea
CC20	M	13	CF at 0.5 m	5 y 4 m	8 y	0.74	Nystagmus, esotropia

Note. M = male; F = female; N/A = not available; FFL = fixing and following light; PL+ = able to perceive light; PR+ = able to report the location of light; CF = counting fingers; CFCF = counting fingers close to face. [a]Positive logMAR values indicate the degree of vision loss, i.e., higher values denote lower visual acuity. [b](Partially) absorbed cataracts. [c] Absorbed cataracts. [d]The presence of nystagmus was not reported in the medical file. [e]Neither retinal glow with retinoscopy nor fundus view with ophthalmoscopy was obtained prior to cataract surgery.

Supplementary table 2. Congenitally blind participant details (adapted from Hölig et al. (2023) [25])

Participant	**Sex**	**Age (years)**	**Visual acuity**	**Cause of blindness**
CB1	M	39	N/A	Microphthalmia OU
CB2	M	21	NLP	Microphthalmia OU, microcornea OU
CB3	F	19	PL^+	Microphthalmia OU
CB4	M	17	PL^+	Phthisis bulbi OD, anterior staphyloma OS
CB5	F	19	PL^+	Anterior staphyloma OD, phthisis bulbi OS
CB6	M	23	CFCF	Corneal scar OU, microphthalmia OU
CB7	M	16	PL^+, PR^+	Microphthalmia OU, band-shaped Keratopathy OU
CB8	F	17	NLP	Leber's congenital amaurosis

Note. M = male; F = female; OU = both eyes; OD = right eye; OS = left eye; N/A = not available; FFL = fixing and following light; NLP = no light perception; PL+ = able to perceive light; PR+ = able to report the location of light; CFCF = counting fingers close to face.

Supplementary table 3. Developmental cataract participant details (adapted from Hölig et al. (2023) [25])

Participant	**Sex**	**Age (years)**	**Cataract onset [a]**	**Pre-surgery visual acuity [b]**	**Age at surgery (y = years, m = months)**	**Time since surgery (y = years, m = months)**	**Visual acuity [b]**
DC1	M	13	Developmental	PL+, PR+	9 y	4 y	1.78
DC2	M	13	Developmental	0.80	12 y 6 m	7 m	0.10
DC3	F	43	Age-related [c]	0.60	40 y 4 m [d]	3 y	0.30
DC4	M	12	Congenital	0.80	11 y 10 m	8 m	0.60
DC5	M	9	Developmental	1.04	7 y 2 m	2 y	0.30
DC6	M	9	Developmental	0.90	7 y	2 y	0.10
DC7	M	17	Developmental	0.40	12 y 6 m	5 y	0.10

DC8	M	13	Developmental	1.00	8 y	5 y	0.20
DC9	M	11	Developmental	0.48	8 y 4 m	4 y	0.30
DC10	F	13	Developmental	0.50	10 y 2 m	3 y	0.10
DC11	F	21	Developmental	0.40	17 y 4 m	4 y	0.20

Note. M = male; F = female; PL+ = able to perceive light; PR+ = able to report the location of light, - = neither nystagmus nor strabismus reported in the medical records. [a] Developmental cataracts typically develop gradually and remain unnoticed for some time; thus, it is not possible to define a clear onset. [b] Positive logMAR values indicate the degree of vision loss, i.e., higher values denote lower visual acuity. [c] The onset of cataracts was after the age of 12 years. [d] Operated only in one eye.

Results

DC vs SC comparisons

DC individuals showed higher MD, RD and AD compared to SC individuals (supplementary figure 1C, supplementary table 4). As with other group comparisons, clusters were primarily seen in visual tracts, which again exhibited higher average tract deviation (MD: 20.39, RD: 16.19, AD: 20.85) than non-visual tracts (MD: 1.80, RD: 2.02, AD: 8.67). More precisely, differences were primarily observed for early visual tracts, namely the left and right OR and the splenium, although the left IFOF also showed differences for all four metrics. As with CC individuals, average tract deviation scores indicated relatively fewer differences between DC and SC individuals for FA (visual: 8.38, non-visual: 1.82), but differences in the left and right ILF may be noteworthy.

Supplementary table 4. Cluster masses and segment ranges for visual tracts of DC vs SC participants.

Metric	L_OR	R_OR	Splenium	L_IFOF	R_IFOF	L_ILF	R_ILF	L_SLF	R_SLF
FA				9.29 [81-84]	11.01 [23-26]	21.62 [77-83] 19.62 [88-95]	13.86 [87-92]		

MD	64.33 [1-18]	34.44 [6-19] 17.44 [23-29]	10.4 [57-60] 29.74 [80-91]	13.61 [60-65]			13.56 [1-6]		
RD	50.56 [1-16]	13.07 [11-15] 9.22 [89-92]	12.94 [70-74] 26.21 [80-90]	9.09 [82-85]	10.75 [23-26]		13.83 [1-6]		
AD	52.79 [1-19] 17.28 [41-47]	20.53 [1-8] 22.46 [13-21] 34.89 [24-38] 9.5 [46-49]	14.89 [93-98]	15.33 [60-65]					

Table note: Each entry refers to a cluster of significantly different segments found in the left or right inferior longitudinal fasciculus, organized by group comparison, hemisphere and tensor metric. Multiple entries refer to multiple clusters. Clusters are reported as 'cluster mass [segment range]'. CC – congenital cataract reversal individuals; CB – Permanently congenitally blind individuals; SC – Normally sighted control individuals; FA – Fractional anisotropy; MD – Mean diffusivity; RD – Radial diffusivity; AD – Axial diffusivity.

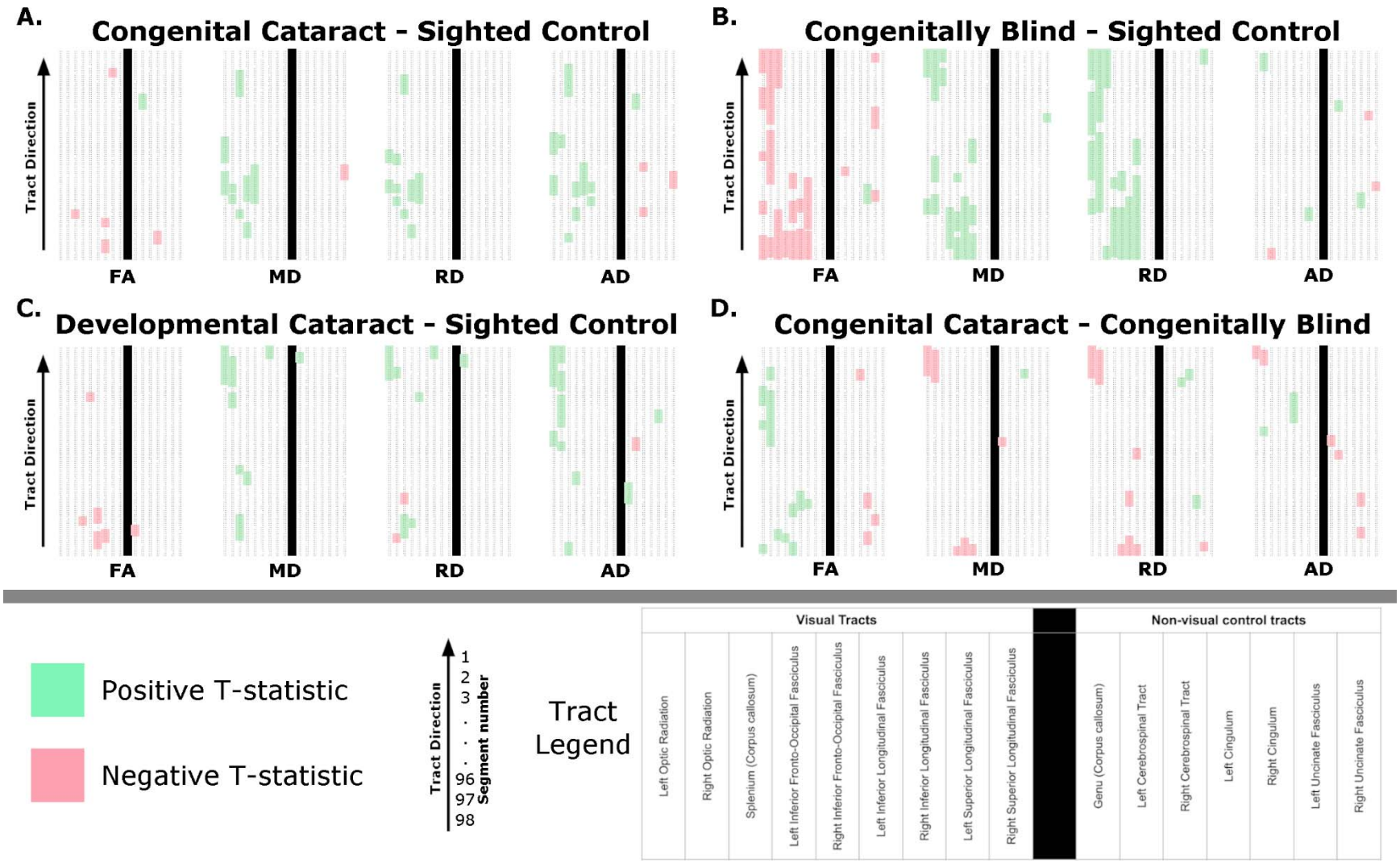

Supplementary figure 1: Overview of significant differences between groups. Each subplot shows significant differences in fractional anisotropy (FA), mean diffusivity (MD), radial diffusivity (RD) and axial diffusivity (AD) (labelled at the bottom). Each column represents a specific tract, for which 98 segments are

displayed in rows, with downstream locations at the top. As indicated in the tract legend, tracts are organized from left to right as follows: Left Optic Radiation, Right Optic Radiation, Splenium, Left Inferior Fronto-Occipital Fasciculus, Right Inferior Fronto-Occipital Fasciculus, Left Inferior Longitudinal Fasciculus, Right Inferior Longitudinal Fasciculus, Left Superior Longitudinal Fasciculus, Right Superior Longitudinal Fasciculus, Genu, Left Corticospinal Tract, Right Corticospinal Tract, Left Cingulum, Right Cingulum, Left Uncinate Fasciculus, and Right Uncinate Fasciculus. The vertical black line indicates the separation of vision-related tracts (left) from non-visual control tracts (right). Clusters ($p < 0.001$) are coloured according to the direction of the difference. For example, in A, congenital cataract reversal individuals vs matched sighted controls, green clusters indicate that the respective tensor metric is significantly greater for the congenital cataract reversal group than for normally sighted controls, while red clusters indicate the opposite. This theme accordingly applies to B, permanently congenitally blind individuals vs matched sighted controls, C, developmental cataract reversal individuals vs matched normally sighted controls, and D, congenital cataract reversal individuals vs permanently congenitally blind individuals.

Correlations with variables of interest

Supplementary table 5: Spearman's rho values for the relationship between age at surgery and mean DTI metrics of visual tracts.

Tract	FA	MD	RD	AD
Left optic radiation	rs = 0.055	rs = -0.124	rs = -0.023	rs = -0.138
Right optic radiation	rs = 0.305	rs = 0.015	rs = -0.060	rs = 0.072
Splenium	rs = 0.028	rs = 0.111	rs = 0.107	rs = 0.221
Left IFOF	rs = 0.346	rs = -0.137	rs = -0.186	rs = 0.162
Right IFOF	rs = 0.312	rs = 0.002	rs = -0.121	rs = 0.150
Left ILF	rs = 0.413	rs = -0.136	rs = -0.243	rs = 0.110
Right ILF	rs = 0.099	rs = 0.106	rs = 0.061	rs = 0.161
Left SLF	rs = 0.259	rs = -0.137	rs = -0.224	rs = 0.357
Right SLF	rs = 0.196	rs = -0.033	rs = -0.153	rs = 0.137

Table note: Spearman's rho values are reported for the correlation between each tract's mean metric values and age at surgery in months. Only congenital cataract reversal individuals were included. No significant correlations were revealed. FA – Fractional anisotropy; MD – Mean diffusivity; RD – Radial diffusivity; AD – Axial diffusivity; IFOF – inferior fronto-occipital fasciculus; ILF – inferior longitudinal fasciculus; SLF - superior longitudinal fasciculus.

Supplementary table 6: Spearman's rho values for the relationship between time since surgery and mean DTI metrics of visual tracts.

Tract	FA	MD	RD	AD
Left optic radiation	rs = 0.181	rs = -0.059	rs = -0.182	rs = 0.086
Right optic radiation	rs = 0.060	rs = -0.297	rs = -0.265	rs = -0.214
Splenium	rs = 0.125	rs = -0.257	rs = -0.251	rs = -0.362
Left IFOF	rs = -0.006	rs = -0.127	rs = -0.120	rs = -0.226
Right IFOF	rs = 0.072	rs = -0.333	rs = -0.237	rs = -0.326
Left ILF	rs = -0.187	rs = -0.048	rs = 0.026	rs = -0.206
Right ILF	rs = 0.096	rs = -0.296	rs = -0.255	rs = -0.295
Left SLF	rs = -0.020	rs = -0.103	rs = -0.059	rs = -0.481*
Right SLF	rs = 0.017	rs = -0.276	rs = -0.109	rs = -0.368

Table note: Spearman's rho values are reported for the correlation between each tract's mean metric values and time since surgery in months. Only congenital cataract reversal individuals were included. AD values in the left SLF were significantly correlated to time since surgery ($p = 0.037$), but this did not survive multiple comparisons correction. FA – Fractional anisotropy; MD – Mean diffusivity; RD – Radial diffusivity; AD – Axial diffusivity; IFOF – inferior fronto-occipital fasciculus; ILF – inferior longitudinal fasciculus; SLF - superior longitudinal fasciculus.

Supplementary table 7: Spearman's rho values for the relationship between visual acuity and mean DTI metrics of visual tracts.

Tract	FA	MD	RD	AD
Left optic radiation	rs = -0.023	rs = -0.001	rs = 0.105	rs = -0.165
Right optic radiation	rs = 0.180	rs = 0.129	rs = 0.069	rs = 0.052
Splenium	rs = 0.373	rs = -0.112	rs = -0.201	rs = 0.006
Left IFOF	rs = 0.233	rs = 0.004	rs = -0.025	rs = 0.176
Right IFOF	rs = 0.226	rs = 0.057	rs = -0.013	rs = 0.050
Left ILF	rs = 0.265	rs = 0.031	rs = -0.085	rs = 0.085
Right ILF	rs = 0.101	rs = 0.065	rs = 0.040	rs = 0.190
Left SLF	rs = -0.075	rs = -0.081	rs = -0.057	rs = 0.086
Right SLF	rs = 0.058	rs = 0.024	rs = -0.041	rs = 0.104

Table note: Spearman's rho values are reported for the correlation between each tract's mean metric values and visual acuity reported as logMAR values (higher values indicate lower visual acuity). Only congenital cataract reversal individuals were included. No significant correlations were revealed. FA – Fractional anisotropy; MD – Mean diffusivity; RD – Radial diffusivity; AD – Axial diffusivity; IFOF – inferior fronto-occipital fasciculus; ILF – inferior longitudinal fasciculus; SLF - superior longitudinal fasciculus.

Discussion

Alterations to white matter in developmental cataract reversal individuals

We consider the DC group to be a control group for the treatment (cataract surgery) rather than an experimental group, e.g., to determine the timing of sensitive periods. The main reasons are: First and foremost, it is important to note that the DC group is extremely variable. Inherently, developmental cataracts happen gradually and can go unnoticed for some time. Thus, defining a time of onset is impossible. Second, as can be seen in supplementary table 3, the majority of participants had some level of vision prior to surgery, as intervention is typically sought prior to complete loss of vision.

Relative to matched sighted controls, we observed increases in MD, RD and AD mostly in the optic radiation and a few differences in FA in the left and right ILF. Changes in the optical radiation were prominent at the occipital terminals of the optic radiation, whereas in CC participants, alterations compared to the SC group were more central in tracts. While we refrain from interpreting the results for the optic radiation of the DC group, we noticed that they qualitatively differed from those of the CC group (location and parameter). Interestingly are the overlaps of FA decreases in the ILF, which seem even more extensive in the DC group. This result could indicate a protracted vulnerability of the ventral occipital cortex in childhood. The

functional consequences are yet unknown. The only existing study on face processing found reliable impairments for CC individuals but not for DC individuals [18].